SM Report 94-2

ADA 279 808

DYNAMIC DECOHESION OF BIMATERIALS : EXPERIMENTAL OBSERVATIONS AND FAILURE CRITERIA

by

J. Lambros and A. J. Rosakis

Graduate Aeronautical Laboratories
California Institute of Technology
Pasadena, CA 91125.

Abstract

Some results of high speed interferometric measurements on dynamically propagating interfacial cracks are presented. PMMA/Steel bimaterial specimens of the one point bend type are used. They are impact loaded using either a drop weight tower device or a high speed gas gun. This results in two distinct groups of experiments at different loading rates. In all cases very high crack propagation speeds are seen. In gas gun experiments, terminal crack tip speeds of up to $1.5C_s^{PMMA}$, where C_s^{PMMA} is the shear wave speed of PMMA, are measured. In addition, high accelerations ($\approx 10^7$g, where g is the acceleration of gravity) are observed and reported. Theoretically predicted near tip fields are used to extract experimental values of the dynamic complex stress intensity factor histories in each test. Using the fitted histories of the complex stress intensity factor, a dynamic crack growth criterion relating the energy release rate to phase angle and crack tip velocity is proposed and discussed.

1 Introduction

The increased use of composite materials in engineering applications in recent decades has become an incentive for extensive research, both basic and applied, into the various failure modes of such materials. It was soon recognized that the macroscopic performance of composite materials was intimately related to effects occurring at the interface between the different phases of the composite. This led to a recent explosion of research in interfacial fracture effects in bimaterial systems.

The first study of interfacial fracture was made by Williams (1959). He found an oscillatory stress singularity present at the tip of a crack lying on an interface between two elastic solids. Until recently, only a few researchers had provided some explicit solutions of the stress field in particular interfacial fracture problems (Sih and Rice (1964), England (1965), Erdogan (1965), and Rice and Sih (1965)). In all these solutions, asymptotically an oscillatory stress singularity was found, confirming Williams (1959) result. The recent resurgence of work on interface fracture has resulted in many more contributions. Most notable are those of Rice (1988), and Shih (1991). Up to this point most of the research activity on interface fracture is on issues regarding the *quasi-static* failure of bimaterial systems. To fully understand the *catastrophic* nature of composite fracture, which is important in many engineering applications, a good understanding of *dynamic* interfacial fracture mechanics is also necessary. Due to the complexity of this problem, however, only a few theoretical investigations have been made so far (Goldshtein (1967), Brock and Achenbach (1973), Willis (1971, 1973), Atkinson (1977), Yang et al. (1991) and Deng (1993)). To our knowledge, only two preliminary experimental studies on this subject are currently available (Tippur and Rosakis (1991) and Liu et al. (1993)).

In the current work we investigate the, essentially unexplored, area of experimental dynamic interfacial fracture mechanics. The general objective sought by this investigation is the understanding of the highly transient dynamic interfacial crack initiation, growth and arrest in bimaterial systems. In particular, in the context of the present paper, it is intended

to provide a summary of recent experimental observations on the issue of dynamic interface fracture, culminating at the proposal of a physically based and accurate criterion for crack initiation and growth in bimaterial systems. Use of high speed photography and interferometric optical diagnostics can provide real time measurements of mechanical fields at the vicinity of initiating and propagating interfacial crack tips. The particular optical method used here is the newly developed method of Coherent Gradient Sensing (CGS). (Tippur et al. (1991), Rosakis (1993)) This is a full field lateral shearing interferometer which has shown great promise in real time imaging of dynamic crack tip fields in homogeneous materials.

2 Experimental procedure

2.1 Coherent Gradient Sensing interferometer (CGS)

The method of CGS was first proposed by Tippur et al. (1991) and is described in detail by Rosakis (1993). The set-up of the method in a transmission configuration for the case of a dynamically loaded bimaterial specimen is shown schematically in figure 1. A coherent, monochromatic, collimated laser beam is incident on the deforming specimen. After transmission through the specimen it acquires an optical path difference and looses collimation. The resulting, now non-collimated, beam passes through two line diffraction gratings G_1 and G_2 of fine pitch p (typically 40 lines/mm). They are situated a distance Δ apart and perform a shearing of the incident wave front as described below. The gratings' output intensity is transmitted through a filtering lens L. A diffraction spot pattern is obtained on the filtering plane, which is located at the back focal plane of the lens L. At this plane all but one diffraction orders are blocked. The one remaining diffraction spot (either of ± 1 orders), shown in figure 1 as the open circle on the filtering plane, is imaged to

produce an interference pattern. For the case of a dynamic experiment the imaging medium is high speed camera focused on the specimen.

If $S(x_1,x_2)$ is the optical path change introduced by the deforming specimen in the transmitted laser beam, then it has been shown by Tippur et al. (1991) that constructive interference will occur on the image plane when

$$\frac{\partial\left(S(x_1,x_2)\right)}{\partial x_1}=\frac{mp}{\Delta}, \qquad m=0,\pm1,\pm2,\ldots \; . \tag{1}$$

If the grating lines are parallel to the x_1 direction then it can be shown that the condition for constructive interference becomes,

$$\frac{\partial\left(S(x_1,x_2)\right)}{\partial x_2}=\frac{np}{\Delta}, \qquad n=0,\pm1,\pm2,\ldots \; . \tag{2}$$

For solid mechanics applications, it is desirable to relate the quantity $S(x_1,x_2)$ to the stress state in the deforming specimen. Such a relation is discussed in detail in Rosakis (1993) and will not be presented here. For a linearly elastic, isotropic material under plane stress conditions, see Lee and Rosakis (1993) for the extent of the plane stress region in a cracked bimaterial specimen, $S(x_1,x_2)$ can be expressed as,

$$S(x_1,x_2)\approx c_\sigma h\left[\hat{\sigma}_{11}(x_1,x_2)+\hat{\sigma}_{22}(x_1,x_2)\right], \tag{3}$$

where c_σ is a stress optical coefficient for the material, h is the specimen thickness and $\hat{\sigma}_{11}$ and $\hat{\sigma}_{22}$ are *thickness averages* of the in-plane stress components in the plate.

Thus for points outside the near tip three dimensional region the CGS patterns assume a simple interpretation in terms of two dimensional stress field approximations. In particular, equations (1) and (2) in conjunction with equation (3) now indicate that the

fringes obtained from regions surrounding the three dimensional zone can be related to the in-plane gradients of $\hat{\sigma}_{11}+\hat{\sigma}_{22}$ as follows

$$c_\sigma h\frac{\partial(\hat{\sigma}_{11}+\hat{\sigma}_{22})}{\partial x_1}=\frac{mp}{\Delta},\qquad c_\sigma h\frac{\partial(\hat{\sigma}_{11}+\hat{\sigma}_{22})}{\partial x_2}=\frac{np}{\Delta},\qquad m,n=0,\pm1,\pm2,\ldots, \tag{4}$$

where in the case of transmission c_σ is the stress optical coefficient of PMMA.

2.2 Bimaterial Experiments

To be able to use a transmission CGS arrangement in our experimentation, one side of the bond, the more compliant side, was chosen to be Plexiglas (Poly-Methylmethacrylate or PMMA). This is a transparent polymer that is easily machined and handled. At room temperature it behaves in a brittle fashion. The other side of the bond was chosen as either 6061-T6 aluminum or AISI 4340 steel, both of which are considerably stiffer and tougher than Plexiglas. Throughout this study, the PMMA side of each specimen will be referred to as material-1 and the metal side as material-2. So with reference to figure 2, the more compliant material occupies the positive x_2 plane. The mechanical properties of the constituents are shown in table 1. Table 1 also shows the value of the plane stress quasi-static oscillatory index, defined later on by equation (7), for the bimaterial combinations of PMMA/aluminum ($\varepsilon^{P/A}$) and PMMA/steel ($\varepsilon^{P/S}$). Also shown is the value of $\varepsilon^{P/R}$ for Plexiglas bonded to a rigid substrate. As can be seen, these three values are extremely close. This would suggest that we can expect intense interfacial effects during the dynamic fracture event. It also suggests that the approach of some researchers (Hutchinson (1989), Nakamura (1991)) to set ε=0 invoking small material mismatch cannot be applied in our case.

The specimen preparation procedure follows the lines of Tippur and Rosakis (1991) and Liu et al. (1993) and will not be described here. The crucial issue of bond strength has been addressed by the performance of bond calibration tests by Tippur and Rosakis (1991).

These tests essentially consist of static tests to measure the fracture toughness of specimens made up of two halves of PMMA bonded together using the procedure described above. It was shown that the fracture toughness of the bonded PMMA specimens was over 95% of that of homogeneous PMMA.

The bimaterial specimens used in the dynamic experiments have either a pre-cut edge notch or a sharp pre-crack of length 25mm along the interface. After the initiation event, a crack propagates dynamically along the interface. The bimaterial specimens are impact loaded in a drop weight tower (Dynatup-8100A) or a high speed gas gun. The transmission CGS technique in conjunction with high speed photography is used to record dynamic crack tip fields around the notch tip (only on the PMMA side of course). A rotating mirror high speed camera (Cordin model 330a) is used. A Spectra-Physics Argon-ion pulse laser (model 166) is used as the light source. By using short pulses of 30ns duration we are able to freeze even the fastest of running cracks and thus produce a sharp interference pattern during crack growth. The interframe time (controlled by the interval between pulses) is typically set at 1μs for a total recording time of 80μs. The laser pulsing is triggered by a strain gauge on the specimen that senses the impact of the drop weight. When it reaches a certain threshold, the laser starts pulsing.

True symmetric one or three point bend loading cannot be achieved since it is extremely difficult to apply the impact load exactly on the interface, which is very thin. In addition since the wave speeds of PMMA and steel are vastly different, the loading history at the crack tip would be completely different if the specimen were impacted on the PMMA or the steel side. Thus it was chosen to impact the specimen a small distance (7mm) into the steel side of the bond. A sequence of high speed interferograms from a PMMA/aluminum test is shown in figure 3 (from Tippur and Rosakis (1991)). This is a three point bend test conducted in a drop weight tower. The impact speed used was 2 m/s. When the crack initiates (t=0μs), intense stress waves emanate from the crack tip. These waves are visible in figure 3 as discrete kinks in otherwise smooth fringes and as circular lines centered at

points along the crack line. This observation is a reliable sign of a highly dynamic event. Indeed, as will be seen later, terminal velocities seem to be about 90% of the Rayleigh wave speed of PMMA, and in fact in some tests they have exceeded it. Similar waves are visible in the interferograms of figure 4. These are from a PMMA/steel drop weight tower one bend experiment, at an impact velocity of 4m/s.

3. Subsonic and intersonic crack growth along bimaterial interfaces

3.1 Experimental observations

Drop weight tower experiments

Figure 3 shows a sequence of dynamic interferograms from a PMMA/aluminum three point bend test (from Tippur and Rosakis (1991)). Time $t=0\mu s$ corresponds to the time of crack initiation. Interferograms at negative times have been taken before initiation. In this figure it can be seen that between $t=-42\mu s$ and $t=0\mu s$ the fringe pattern surrounding the initial notch tip grows in size and also rotates with respect to the notch line. The size of the fringe pattern at each time depends on the magnitude of the stress field around the tip. The particular orientation of each lobe of the pattern is dependent on the relative amounts of opening and shearing stresses around the tip (i.e., the stress mixity). It is clearly visible that before initiation the pattern surrounding the notch tip changes in both size and orientation. In contrast, after crack initiation the fringe pattern stays relatively uniform, signifying that some fundamental physical quantities, such as stresses or crack face displacements, must remain constant during crack propagation. Such behavior is typical of all tests performed in under the drop weight tower device.

After the specimen is impacted, on the metal side, a compressive stress wave travels the vertical width of the specimen. It is reflected as a tension wave from the traction free

end on the bottom of the plate. Although impact is always on the side of the metal, impact waves are also generated in the PMMA side because of the existence of the bond. However, waves in the metal side travel much faster than in the PMMA side so the wave generated upon impact reaches the notch tip from the metal side first. The tip is thus loaded by subsequent arrivals of reflected waves from other boundaries of the metal plate. A time of about 75-80μs passes between the time of impact and the time of crack initiation. In this time no waves traveling in the PMMA have reached the notch tip. All deformation effects visible in the interferograms of the PMMA side are from leakage of energy from the metal side to the PMMA through waves crossing the interface. Essentially throughout all tests, *the crack is driven by the metal side of the bond.* This will become even more obvious in the subsequent analysis of the high speed gas gun experiments.

After the crack initiates intense stress waves are emanated from the crack tip. These waves are visible in figures 3 and 4 as discrete kinks in otherwise smooth fringes. This observation is a reliable sign of the existence of very strong dynamic effects and of high velocities of crack growth that are a large fraction of the Rayleigh wave speed of PMMA (c_R^{PMMA}). It should be noted that such waves are not usually visible after crack initiation in homogeneous PMMA specimens of the same configuration and loading, where the observed maximum crack tip speeds are around $0.35\,c_R^{PMMA}$. However, such waves do appear in optical CGS or caustic patterns of growth in high strength materials (see Rosakis (1993)), when crack tip speeds are in excess of $0.4\,c_R^{PMMA}$.

The actual crack tip speed and acceleration histories corresponding to the PMMA/steel experiment shown in figure 4 are plotted in figures 5(a,b). The crack tip speed increases to its largest value in a very short time (~15μs). This is also evident by the presence of large crack tip accelerations at the beginning of crack growth. Consistent with the observation of stress waves during crack growth is the measured maximum crack tip speed. This is seen to be around 800m/s or $0.85\,c_R^{PMMA}$. This observation was rather surprising given previous experience with dynamic crack growth in homogeneous PMMA

specimens of the same configuration and loading (maximum speeds of ~$0.35 c_R^{PMMA}$). Attributing the phenomenon of high crack tip speeds to the existence of a weak bond is not very convincing since the bond calibration technique revealed a bond fracture toughness very close to that of PMMA (see Tippur and Rosakis (1991)). In fact a strong bond is *necessary* in order to drive the crack tip to higher speeds. It is already obvious in these experiments that energy transfer across the interface from the metal side is responsible for crack initiation and growth, simply because in the time frames involved very little wave motion occurs in PMMA. A strong bond is necessary because otherwise less energy would be transferred and the crack tip would not be able to propagate as fast. This fact will become even more obvious in the higher loading rate experiments described later. In addition we believe that these effects of energy transfer are more pronounced because of the large mismatch of elastic properties between PMMA and steel (or aluminum).

One noteworthy point is that the values of acceleration quoted in figure 18(b) are not meant to be exact quantitative results. They are products of two differentiations of the crack length history and are susceptible to error. Nevertheless these values shed light into the orders of magnitude of acceleration encountered in such an experiment.

Gas gun experiments

Because of the intrinsic difficulties associated with the problem of dynamic interfacial fracture, few theoretical studies have been performed (Goldshtein (1967), Brock and Achenbach (1973), Atkinson (1977), Willis (1971,1973)). Even so, it should be noted that there is a disagreement on the theoretically predicted value of the terminal velocity for dynamically propagating interfacial cracks. Atkinson (1977) claimed a terminal velocity equal to the lower of the Rayleigh wave speeds of the two constituents. In contrast Willis (1973) argued that the terminal velocity was a little greater than the lower of the two Rayleigh wave speeds. More recently the problem of dynamic interfacial crack growth has been studied by Yang et al. (1991). They provided an asymptotic solution for the stress

field surrounding the tip of a dynamically propagating bimaterial crack. One very important conclusion of their study is that as the crack tip velocity approaches the lower of the two Rayleigh wave speeds a finite amount of energy has to be transmitted to the crack tip to maintain extension at $c_R^{(1)}$ with non-zero complex stress intensity factor. This is unlike the homogeneous case where an infinite amount of energy has to be transmitted to the crack tip to maintain extension at c_R if the stress intensity factor is non-zero (Broberg (1960) and Freund (1990)). This obviously makes it energetically impossible for a crack in a *homogeneous* solid to exceed the material's Rayleigh wave speed, but apparently no such restriction exists in the bimaterial case.

As was seen in figure 5, experimental measurements from the drop tower tests resulted in crack tip speeds close to c_R^{PMMA} (the lower Rayleigh wave speed). In fact towards the end of our observation window, the velocity seemed to rise further. Since no energetic restrictions exist for the bimaterial case, we believed that it would be possible to drive the interfacial crack to higher speeds by subjecting the specimen to different loading histories resulting in higher rates of loading. Use of a high speed gas gun and a one point bend loading configuration were made to produce loading rates in cracked bimaterial plates that were higher than those encountered in drop weight tower experiments. The gas gun projectile was made out of steel. It was 50mm in diameter and 75mm in length and the impact velocity used was 20m/s. A sequence of selected interferograms from such a test is shown in figure 6. In this test a sharp starter crack was used. The resulting crack tip speed and acceleration histories for this particular test are shown in figures 7(a,b). It is clear that the Rayleigh wave speed of Plexiglas (c_R^{PMMA}) has been exceeded by the crack tip. In addition the shear wave speed of Plexiglas has also been exceeded. After the shear wave speed of PMMA has been exceeded the crack seems to decelerate to a constant speed around 1100m/s. This feature of the plateau in the crack tip speed history was also seen in several other gas gun tests. The reason for this deceleration and constant speed is not yet clear and is still being investigated. In any case it is a very repeatable feature of the

experimental measurements. At later times, though, the crack tip speed increases even further, but unfortunately the growing crack exits the window of our observation.

When a specimen containing a *blunt* starter notch was impacted with the gas gun projectile, recorded terminal crack tip speeds were even higher than those seen in figure 7; in some cases approaching the longitudinal wave speed of PMMA. A sequence of interferograms from such an experiment is shown in figure 8. The corresponding crack tip speed history for this test is shown in figure 9. Here the maximum crack tip speed is estimated to be about 85%-90% of the plane stress dilatational wave speed of PMMA. Visual evidence of crack propagation in the intersonic regime for PMMA can also be seen in the interferograms in figure 8. (Recall that only the PMMA side, which is transparent, is visible). A clear change of the nature of the fringe pattern occurs between the first and last frames of figure 8. Initially, in the first one or two frames, the fringes are smooth and continuous. Within a few microseconds, the main lobe of the fringe pattern becomes squeezed and the fringes develop distinct kinks along certain directions. In the last interferogram of figure 8 the kinks have merged into "shock like" formations. It is not clear at this time exactly what these kinks represent. Since the crack is traveling at a velocity in the intersonic range for PMMA, we would expect shear, but not dilatational, shock waves to be present. Unfortunately because the optical technique of CGS measures gradients of direct stress components, shear effects cannot be imaged. It is believed that the apparent "shock" formations in the later interferograms either form because of Head waves, that are propagating in front of the crack tip, or are three dimensional effects associated with non-straight propagation of the crack front. This subject is still under investigation and will be presented in Lambros et al. (1994).

These observations are very interesting because, to our knowledge, no direct observations of unassisted intersonic or supersonic crack propagation have ever been made in homogeneous materials, even though a large number of theoretical studies exist on the subject (e.g., the contributions of Burridge et al. (1979) and more recently of Broberg

(1985, 1989), Bykovtsev and Kramarovskii (1989), Aleksandrov and Smetanin (1990) and Broberg (1993)). In the work of Broberg (1985) some indirect evidence is presented that shows that in certain earthquake sliding events, intersonic crack growth velocities may be possible.

In experiments involving gas gun loading the observed crack initiation time was about 30μs after impact. This is much less than the 80μs of the previous drop weight tower experiments. It also correlates well with the time it takes a compressive dilatational wave to travel the width of the specimen, reflect off the traction free bottom surface of the metal side and reach the tip once again. This reinforces the argument that the whole crack growth process in these experiments is driven by the metal side of the bond, via leakage of energy across the interface. It is believed that it is an excess supply of this energy that causes the crack tip to be driven at speeds that are intersonic for PMMA, but still below the Rayleigh wave speed of steel.

3.2 Data reduction and results

In the work of Tippur and Rosakis (1991) use of the quasi-static plane stress asymptotic stress field was made when extracting data from dynamic interferograms. Obviously this is not a correct approach, since it is clear that large dynamic and transient effects occur in dynamic interfacial fracture. However, that was the only theoretical result available at the time. Since then a few researchers (Yang et al. (1991), Wu (1991), Deng (1992,1993)) have determined the spatial structure of the near tip stress field around a bimaterial crack, propagating dynamically under plane stress and steady state conditions. In addition, a higher order transient analysis for a dynamically propagating crack has been obtained by Liu et al. (1993). As may be necessary, one can use either the asymptotic or the higher order transient stress fields to extract the relevant fracture parameters. The procedures have been described in Rosakis et al. (1991) and Liu et al. (1993). Here we shall discuss briefly the fitting procedure using the asymptotic result of Yang et al. (1991)

which can be used with interferograms exhibiting some region of dynamic K^d-dominance. (A region surrounding the crack tip in which the stress field is well described by the most singular term of the asymptotic expansion for stress is called a K^d-dominant region).

For interfacial cracks propagating dynamically under steady state conditions in bimaterial specimens Yang et al. (1991) observed that near the crack tip the stress field assumes the form,

$$\sigma_{\alpha\beta} = Re\left\{\frac{K^d r^{i\varepsilon}}{\sqrt{2\pi r}}\right\}\tilde{\sigma}^{(1)}_{\alpha\beta}(\theta,v) + Im\left\{\frac{K^d r^{i\varepsilon}}{\sqrt{2\pi r}}\right\}\tilde{\sigma}^{(2)}_{\alpha\beta}(\theta,v)\ , \tag{5}$$

where r, θ are polar coordinates of a coordinate system *translating* with the crack tip at speed v and $K^d = K^d_1 + iK^d_2$ is the *complex dynamic* stress intensity factor. Analytical expressions for $\tilde{\sigma}^{(1)}_{\alpha\beta}$ and $\tilde{\sigma}^{(2)}_{\alpha\beta}$ are given in Yang et al. (1991). Unlike the quasi-static case, the oscillatory index, ε, which is a material mismatch parameter, is now a function of crack tip speed as well as of the moduli of the materials of the bimaterial combination (i.e., $\varepsilon = \hat{\varepsilon}(v)$).

The field quantity of interest in analyzing the CGS fringe patterns for PMMA is $ch\partial(\hat{\sigma}_{11} + \hat{\sigma}_{22})/\partial x_1$ (see equation (4)). By differentiating equation (5) with respect to x_1 and after some algebraic manipulation, we have

$$\begin{aligned} ch\frac{\partial(\hat{\sigma}_{11}+\hat{\sigma}_{22})}{\partial x_1} = \frac{chr_1^{-3/2}e^{-\varepsilon(\pi-\theta_1)}A}{2\sqrt{2\pi}}\Bigg[& -(1+\alpha_s^2-2\eta\alpha_s)e^{2\varepsilon(\pi-\theta_1)}\cos\left(\frac{3\theta_1}{2}-\phi-\varepsilon\ln r\right) \\ & -(1+\alpha_s^2+2\eta\alpha_s)\cos\left(\frac{3\theta_1}{2}+\phi+\varepsilon\ln r\right) \\ & +2\varepsilon(1+\alpha_s^2-2\eta\alpha_s)e^{2\varepsilon(\pi-\theta_1)}\sin\left(\frac{3\theta_1}{2}-\phi-\varepsilon\ln r\right) \\ & -2\varepsilon(1+\alpha_s^2+2\eta\alpha_s)\sin\left(\frac{3\theta_1}{2}+\phi+\varepsilon\ln r\right)\Bigg], \end{aligned} \tag{6}$$

where

$$A=\frac{\left(\alpha_1^2-\alpha_s^2\right)\left|K^d\right|}{\left(4\alpha_1\alpha_s-\left(1+\alpha_s^2\right)^2\right)\cosh(\varepsilon\pi)},$$

$$\alpha_{1,s}=\left(1-\frac{\dot{a}^2}{c_{1,s}^2}\right)^{1/2},\quad \theta_1=\tan^{-1}\left[(\alpha_1 x_2)/x_1\right],\quad r_1=\sqrt{x_1^2+\alpha_1^2 x_2^2},$$

$$K^d(t)=K_1^d(t)+iK_2^d(t),\qquad \phi(t)=\tan^{-1}\left(K_2^d(t)/K_1^d(t)\right).$$

$c_{1,s}$ are the longitudinal and shear wave speeds respectively and $0\le\theta\le\pi$. One note to be made here is that to obtain the stress field in the lower material we need to substitute $-\pi$ for π in equation (6). In the present study though we only obtain interferograms from the deformation of material-1 (PMMA) so this need not be done.

Parameters $\varepsilon=\hat{\varepsilon}(v)$, $\eta=\hat{\eta}(v)$, are functions of crack tip speed and material properties. ε and η are two mismatch parameters that characterize the interface. They are derived explicitly in Yang et al. (1991) . Parameter ε is given by

$$\varepsilon(v)=\frac{1}{2\pi}\ln\left(\frac{1-\beta(v)}{1+\beta(v)}\right),\quad \text{with}\quad \beta(v)=-H_{12}\left(H_{11}H_{22}\right)^{-\frac{1}{2}},\tag{7}$$

where β is the second Dundurs' parameter characterizing the bimaterial problem (see Dundurs (1969)). Functions $H_{\alpha\beta}$ depend on the elastic properties of the two constituents of the interface and the crack tip velocity v. They are explicitly stated in Yang et al. (1991).

The variation of ε and η with crack tip speed is shown in figures 10 and 11 respectively. Both these figures are for a PMMA/steel bimaterial combination. The plots are for crack tip speeds below the Rayleigh wave speed of Plexiglas, which is the regime in which equation (5) is valid. The parameters are such that $\varepsilon\to\varepsilon_s$, $\eta\to 1$ as $v\to 0$ and equation (5) reduces the quasi-static result of Rice (1988) for $v=0$. ε_s is the *quasi-static* oscillatory index.

In the above relation only the values of the dynamic complex stress intensity factor and the crack tip speed are undetermined by the asymptotic analysis. The crack tip speed is an external parameter that must be furnished by separate experimental measurements. In our case these measurements are made by recording the crack length variation with time. We can use equation (6) to extract K^d as a function of time from optical interferograms by a performing a least squares fitting procedure. From the above discussion it becomes obvious that extraction of parameters like K^d is possible *provided* that experimental data are gathered from a region near the moving crack tip characterized by the structure presented in equations (5) and (6), i.e., that there exists a region of K^d-dominance. However in the case that no region in the specimen is characterized by such a K^d-field, the use of a higher order analysis is mandated as described in Liu et al. (1993). The least squares fitting procedure utilized in this study is very similar to that used in Mason et al. (1992) or Rosakis (1993) and in the interest of brevity will not be described here. One point to note though is that when analyzing optical data, care must be taken to use only data points r_i, θ_i from a region of the specimen that does indeed approximate two dimensional plane stress conditions, if we wish to use equations (4) and (6) to interpret the experimental results. The region in which such conditions are valid in a three point bend bimaterial specimen was determined by the finite element numerical analysis of Lee and Rosakis (1993). Selection of data points was made on the basis of the results of this analysis.

The variation of stress intensity factors K_1^d and K_2^d for the PMMA/steel drop weight tower test presented in figure 4, are shown in figures 12(a,b). The energy release rate G and phase angle ϕ for the same test are shown in figures 13(a,b). G for the case of dynamic interfacial crack growth is given by (Yang et al. (1991)),

$$G = \frac{F}{4\mu_1}|K|^2, \tag{8}$$

where F is a function of velocity and bimaterial system material properties shown explicitly in Yang et al. (1991). Note that F is finite at the Rayleigh wave speed of Plexiglas. The phase angle in figure 13(b) has been calculated from

$$\phi = tan^{-1}\left(\frac{K_2^d}{K_1^d}\right). \tag{9}$$

This implies that a length scale of 1m has been used in this particular plot. The phase angle ranges from $-\pi$ to π to cover all possible sign combinations of K_1^d and K_2^d.

On all plots in figures 12 and 13 $t=0\mu s$ corresponds to the estimated time of crack initiation. Pre-initiation values of K_1^d and K_2^d were determined by fitting the quasi-static stress field of Rice (1988) to interferograms before $t=0\mu s$. Unfortunately determining the time of initiation in each test is not an absolute science. It was observed that when fitting a K^d-field to pictures a few microseconds after $t=0\mu s$ the fit was good only on the outer most fringes. This is contrary to what would be expected at first glance, on the basis of asymptotics. An example of such a case is shown in figure 14 for the interferogram corresponding to $t=2\mu s$ for the experiment shown in figure 4. The diamond points are data points digitized from the interferogram, and the solid line is the result of the fit of equation (6) to those same points. It can be seen that the three outer fringes are in very good agreement with the K^d-dominant fit, while the inside fringes are not. Gradually as time progressed (2-10μs) the quality of the fit deteriorated from the inside out until all K^d-dominance was lost. The gradual collapse of the K^d-field between pictures agreed reasonably well timewise with a dilatational wave being emitted from the crack tip and traveling radially outwards. Such waves would indeed start being emitted when the crack tip initiated. They would travel outwards and destroy the K^d-field that was established in the pre-initiation stages of the experiment. It was possible to determine the time of initiation by choosing the interferogram immediately before the first sign that the innermost fringe

did not conform to a K^d-dominant field, i.e., just before the emission of a wave from the crack tip. Even so there is some uncertainty in the exact time of crack initiation, based on when the crack is visually seen to propagate. This uncertainty is represented in figure 12 and 13 as being between the two dotted vertical lines.

It can be seen in figure 12(a,b) that both K_1^d and K_2^d increase to a maximum value and then sharply drop, with K_1^d attaining negative values towards the end of the test. The energy release rate (figure 13(a)) also increases to a peak a little after $t=0\mu s$ and then drops to a value close to zero implying that the process of dynamic crack propagation along interfaces is highly unstable. This result is corroborated by the steep rise of the crack tip speed in very short times. The continuing increase of G for a short time after crack initiation is related to the fact that a material particle away from the crack tip is not aware of initiation until stress waves emitted from the tip reach it. This effect was illustrated in figure 14. It has also been observed by other researchers. For example, Aoki and Kimura (1993) in a numerical investigation using synthetic caustic patterns at the tip of a crack, observed an overshoot of the measured G just after initiation. On the other hand the phase angle ϕ increases throughout the test. In equation (6) it was seen that in the theoretically predicted stress field from the Yang et al. (1991) K^d-dominant analysis velocity v and phase angle ϕ have complimentary effects since they are both inside the argument of the cosine function. (v enters the cosine through the velocity dependence of ε). Since both v and ϕ are seen to vary considerably throughout crack propagation, but the size and orientation of the observed fringe pattern around the tip seems unchanged (see figures 3 and 4), the two quantities have to be linked in some way as to keep the stress gradients resulting from equation (6) constant. This fact will be exploited further in the next section to propose a possible dynamic crack growth criterion for interfacial fracture.

Because of the presence of oscillatory terms in the stress field shown in equation (6) all inconsistencies associated with the theory of static linear elastic interfacial mechanics

are still present. Of paramount importance is the inconsistency of predicted interpenetration of the crack faces. The extent of the resulting contact zone is given by,

$$r_c = e^{\frac{-\pi/2-\phi+\tan^{-1}(2\varepsilon)}{\varepsilon}}. \tag{10}$$

To accept the measured values of G and ϕ as accurate we must make sure that the extent of predicted contact is much smaller than the smallest characteristic length of the problem and is embedded in the three dimensional region of deformation. Only in that case can the K^d-field surrounding the crack tip control the fracture process. From figure 10, which shows the variation of ε with crack tip speed for a PMMA/steel system, it can be seen that as $v \to c_R^{PMMA}$, $\varepsilon \to +\infty$. As v, and consequently ε, gets larger it would seem that the predicted contact zone r_c would become unacceptably large. When calculating r_c though from experimental measurements it was found that the variation of ϕ suppressed the increase of the contact zone size keeping it at very low values for all but the highest crack tip velocities. An idea of the size of the contact zone predicted for the one point bend PMMA/steel test of figure 4, is given in figure 15. The solid lines are contours of constant contact zone as derived from equation (10) for a range of v and ϕ. The diamond points are the calculated experimental results. Clearly values of the contact zone are below 10^{-4}m. This is well within the zone of three dimensional deformation surrounding the crack tip whose maximum extent is around 2mm.

4. A criterion for dynamic interfacial crack growth

A sequence of dynamic interferograms obtained from the tip of a crack lying along a PMMA/aluminum interface was shown in figure 3. Pre- and post- initiation pictures were shown. As was pointed earlier, before crack initiation ($t<0\mu s$) the fringe pattern around the tip changes both in size and orientation, denoting a change in the energy release rate G and

phase angle ϕ. A variation was indeed seen in the measured values of G and ϕ at times before $t=0\mu s$, for the PMMA/steel drop weight tower test seen in figure 4. In contrast, after initiation, the fringe pattern surrounding the crack does not change significantly with time. The implication of this visual observation is that some fundamental physical quantity, such as stress or crack opening displacement, must remain constant throughout the crack growth phase. It has already been established that v, ϕ and G (or $|K^d|$) all vary considerably during crack growth. Therefore, if we wish to mathematically model the fact that the fringe pattern during crack growth does not change, we must employ some *combination* of these three quantities that remains constant.

It was seen from figure 15 that the variations of v and ϕ were such as to keep the size of the predicted contact zone small throughout each test. This suggests that there is a separate link between v and ϕ during crack growth. In figure 15 it is clearly visible that the diamond points (corresponding to experimental results) curve to the right, denoting an increase in both v and ϕ as the crack grows. We intend to investigate whether the particular path of v and ϕ in each experiment is such as to maintain some fundamental quantity constant. A candidate for such a quantity would be something that does not involve $|K^d|$. We will look into the ratio of the opening (δ_2) to shearing (δ_1) displacements behind the crack tip as one possible candidate. With reference to the geometry of figure 2 δ_1 and δ_2 are defined as

$$\delta_\alpha(r) = u_\alpha(r,\theta=+\pi) - u_\alpha(r,\theta=-\pi), \quad \alpha = 1,2, \tag{11}$$

where $u_\alpha(r,\theta)$ is the displacement field surrounding the crack tip. Figure 16 shows a geometrical representation of δ_1 and δ_2 behind the crack tip. A positive δ_2 means an opening displacement, and a positive δ_1 represents sliding of material-1 along the positive x_1 axis. From the asymptotic analysis of Yang et al. (1991), the crack face displacements are given by,

$$\delta_1(r) = \frac{H_{22}}{\cosh(\pi\varepsilon)}\sqrt{\frac{2r}{\pi}}\frac{|K^d|}{\sqrt{1+4\varepsilon^2}}\frac{1}{\eta}\sin\left(\phi + \varepsilon \ln r - \tan^{-1}(2\varepsilon)\right),$$

and (12)

$$\delta_2(r) = \frac{H_{22}}{\cosh(\pi\varepsilon)}\sqrt{\frac{2r}{\pi}}\frac{|K^d|}{\sqrt{1+4\varepsilon^2}}\cos\left(\phi + \varepsilon \ln r - \tan^{-1}(2\varepsilon)\right).$$

Quantities ε and η have been previously defined and the function H_{22}, which is a function of material properties and crack tip speed, is given in Yang et al. (1991). Each of the two displacements in equation (12) depends on $|K^d|$, but their ratio is only a function of v and ϕ. It is given by,

$$\frac{\delta_1}{\delta_2}(r) = \frac{1}{\eta}\tan\left(\phi + \varepsilon \ln r - \tan^{-1}(2\varepsilon)\right). \tag{13}$$

If we assume that throughout propagation this ratio remains constant, say at a value C_1, at a fixed distance, say a, behind the crack tip, then equation (13) defines a single line in the v, ϕ plane. The equation of this line is given by,

$$\left.\frac{\delta_1}{\delta_2}\right|_{r=a} = C_1 = \frac{1}{\eta}\tan\left(\phi + \varepsilon \ln a - \tan^{-1}(2\varepsilon)\right),$$

or solving for ϕ,

$$\phi = \tan^{-1}(\eta C_1) + \tan^{-1}(2\varepsilon) - \varepsilon \ln a. \tag{14}$$

The dependence of ϕ on v comes in through the velocity dependence of the oscillatory index ε and the traction resolution factor η. (See figures 10 and 11 for the variation of ε and η with v respectively).

In figure 17, which is a plot in the (ϕ, v) plane, the experimental results of the measured crack tip speed v and calculated phase angle ϕ are shown as diamonds. These results are from the PMMA/steel one point bend experiment conducted under drop weight tower impact at 4m/s which was illustrated in figure 4. The solid line in figure 17 represents the curve given by equation (14) that best fits the experimental values. It was decided to evaluate equation (14) at a distance $a=2mm$, which is approximately the innermost radius of the region of K^d-dominance observed in most interferograms. This means that it is also the point closest to the crack tip where equation (14) is valid. The computed ratio δ_1/δ_2 for this fit is $C_1=-0.3$. From figure 17 it seems that indeed throughout crack propagation the quantity δ_1/δ_2 at 2mm behind the *moving* crack tip remains a constant. The amount of crack face opening is 3.3 times the amount of crack face sliding, thus indicating growth at a primarily opening mode *at this particular distance behind the tip.* The choice of a as being 2mm is not crucial for this result. At a different distance behind the tip, the ratio of shearing to opening displacements would again be constant. Because of the nature of the interfacial field, however, the numerical value of this constant would not be the same. But the results presented in this work would still hold.

The condition of a constant δ_1/δ_2 behind the crack tip, equation (14), cannot constitute a dynamic crack growth criterion on its own because it does not predict the magnitude of the stresses surrounding the propagating crack. It may form part of a propagation criterion that relates the phase angle with the crack tip speed. The size of the stress field, and the CGS fringe pattern, surrounding the crack tip is primarily dependent upon $|K^d|$, the magnitude of the complex stress intensity factor. The second part of a fracture criterion would thus have to involve a link between $|K^d|$ (or G), v and ϕ. Consider a constant crack opening displacement, say of value C_2, at the same distance a behind the crack tip as before. From equation (12b) this can be expressed as

$$\delta_2(a) = \frac{H_{22}}{\cosh(\pi\varepsilon)}\sqrt{\frac{2a}{\pi}}\frac{|K^d|}{\sqrt{1+4\varepsilon^2}}\cos\left(\phi + \varepsilon \ln a - \tan^{-1}(2\varepsilon)\right) = C_2,$$

or solving for $|K^d|$

$$|K^d| = C_2\frac{\sqrt{1+4\varepsilon^2}\cosh(\pi\varepsilon)}{H_{22}}\sqrt{\frac{\pi}{2a}}\frac{1}{\cos\left(\phi + \varepsilon \ln a - \tan^{-1}(2\varepsilon)\right)}. \tag{15}$$

The above is a relation between $|K^d|$, v and ϕ with C_2 and a as parameters. For specific values of C_2 and a equation (15) represents a surface in the $|K^d|$, v and ϕ space. An example of such a surface in the G, v, ϕ space (by using equation (8)) is plotted in figure 18 with $a=2mm$ and $C_2=1N/m^2$ (arbitrary).

We can now combine equations (14) and (15) to propose a complete criterion for dynamic crack growth along bimaterial interfaces. Substituting in equation (15) for ϕ from equation (14) we obtain a relation between $|K^d|$ and v only which incorporates the fact that δ_1/δ_2 is constant. The combination of (14) and (15) yields,

$$|K^d| = C_2\frac{\sqrt{1+4\varepsilon^2}\cosh(\pi\varepsilon)}{H_{22}}\sqrt{\frac{\pi}{2a}}\frac{1}{\cos\left(\tan^{-1}(C_1\eta)\right)}. \tag{16}$$

The above depends on constants C_1 and C_2. Dependence on parameter a comes in only through its necessity in the choice of a constant C_1 to fit the experimental data using equation (14), as was done in figure 17. The value of C_1 is then fixed after performing this fit. For the results shown in figure 17 it was seen that $C_1=-0.3$. Unfortunately constant C_2, which essentially is the opening strength of the bond, cannot be easily determined. It can be eliminated though by normalizing equation (16) with some reference value. If we assume that one of the experimentally obtained data points, with parameters v_0, ε_0, η_0, H^0_{22} $|K^d_0|$ and G_0, follows equation (16) then we can eliminate C_2 by computing $|K^d|/|K^d_0|$ as

$$\frac{|K^d|}{|K_0^d|} = \frac{\sqrt{(1+4\varepsilon^2)}\cosh(\pi\varepsilon)H_{22}^0\cos(\tan^{-1}(C_1\eta_0))}{\sqrt{(1+4\varepsilon_0^2)}\cosh(\pi\varepsilon_0)H_{22}\cos(\tan^{-1}(C_1\eta))}. \tag{17}$$

The above result can be converted to a ratio of energy release rates G/G_0 by using equation (8). Comparison with all other experimental points is then possible by plotting the equivalent of equation (17) in the G, v plane.

For the PMMA/steel drop weight tower test used previously, a comparison of the experimental data with equation (17) is shown in figure 19. The normalizing point used is the one corresponding to $v=180m/s$. This point is forced to agree with the computed curve (solid line in figure 19) since it has been used to eliminate the constant C_2. Nevertheless, the remaining points are not forced to follow the curve. It can be seen though that agreement is very good. A notable issue here is that the line in figure 19 is *not* a fit to the experimental values. Only C_1 is fitted to the experimental values using equation (14) as described above. Once this is done the curve given by equation (17) is *completely* specified. This implies that indeed not only is the ratio δ_1/δ_2 constant behind the crack tip, but δ_2 itself is constant. These two facts therefore constitute the proposed dynamic fracture criterion for interfaces. An interfacial crack that has been impact loaded will initiate dynamic propagation at certain critical values of G_c and ϕ_c as is suggested by the work of Liechti and Chai (1991; Liechti and Chai (1992). Subsequently propagation will be such as to maintain δ_1/δ_2 and δ_2 constant at a critical distance behind the moving crack tip. Alternatively, the proposed criterion can be viewed as critical opening (δ_2) and shearing (δ_1) displacements at some distance a behind the moving crack tip. This is equivalent to requiring a self-similar crack profile throughout crack growth.

A possible path in G, v, ϕ space followed during interfacial crack growth that obeys the above proposed criterion is seen in figure 18. As was mentioned above, this surface represents the result of equation (15). For $v=0m/s$ it reduces to the usual "U" shaped curve

that has been observed in quasi-static experiments by Liechti and Chai (1991). This serves as an initiation condition for the case of impact loading. The currently proposed criterion therefore will act as follows :

1.- When the stress field surrounding the stationary crack tip reaches a critical value of G_c and ϕ_c (or equivalently δ_1^c and δ_2^c) then crack initiation occurs.

2.- Subsequently the dynamically growing crack will always propagate in such a way as to keep $\delta_1(t)$ and $\delta_2(t)$ behind it constant at their initiation values. This is equivalent to maintaining a constant crack profile. Such a path is shown on the surface of figure 18 as the line on the surface curving to the right. The projection of this line on the v, ϕ plane will be the contour of constant δ_1/δ_2 seen in figure 17.

Finally, a very important point to note is that although the proposed criterion was derived using the results of the complex stress intensity factor history, the criterion itself may be general enough not to require K^d-dominance in its application. The criterion of a critical crack tip opening displacement, or opening angle, has been used extensively in the past for the fracture of homogeneous solids. It has been seen to be equivalent with initiation criteria based on K_I or J_I and growth criteria (quasi-static or dynamic) based on K_I in situations where K-dominance was assured. However, a criterion based on crack tip opening displacement has also been found to control fracture in instances when K_I or J_I are invalid or cannot be defined, such as growth in elastic-plastic materials. We therefore strongly believe that the proposed criterion for dynamic interfacial crack growth based on both opening and shearing displacements behind the crack tip (crack profile) will be valid in a wide array of cases as well; even if a K^d-dominant region cannot be found.

In general, though the particular numerical values obtained in this study should be critically accepted, the trends indicated seem well founded and logical. Clearly more tests are required, using a wider array of loading geometries and loading rates, to obtain a complete understanding of the phenomena involved in dynamic interfacial fracture. This is currently underway and the results will be reported in a future publication dealing

exclusively with interfacial crack growth criteria. Nevertheless, we believe that a dynamic propagation criterion involving critical displacements behind the crack tip is both reasonable and accurate, and should be investigated further. For a more extensive discussion of the proposed fracture criterion see Lambros and Rosakis (1994).

The concept of a crack growth criterion for dynamic interfacial fracture has also been investigated numerically by Lo et al. (1993). More recent results of their work, that appear in the same special issue of this journal, discuss a comparison of the current experimental results to a numerical simulation of our experiments (see Nakamura et al. (1994)).

5. Conclusion

Very large dynamic effects were observed in all dynamic bimaterial tests. In the case of the high speed gas gun experiments, a terminal crack propagation velocity around 90% of the plane stress dilatational wave speed of PMMA was observed. Because of the very short duration of the experiments in this study, it may be concluded that the whole process of interfacial crack initiation and growth in these tests is driven by energy "leaking" from the metal side to the PMMA side of the bond. It is believed that this fact, enhanced by the large elastic property mismatch of the constituents of the bimaterial system, is what causes the high dynamic nature of these tests. In addition to dynamic effects, very severe transient effects have been seen to occur, especially during the early stages of crack growth. Evidence of transience are the very large accelerations recorded (maximum values of the order of $10^7 g$ where g is the acceleration of gravity). The phenomenon of the existence of highly transient deformations was corroborated by direct comparison of the experimental results to a transient elastodynamic analysis in the work of Liu et al. (1993).

It was experimentally observed that the crack profile (opening and shearing displacements at a given distance behind the propagating crack tip) remained constant

throughout propagation. This observation formed the basis of the proposed dynamic fracture criterion. The use of the notion of an invariant crack face profile as a fracture criterion is both physically sensible and consistent with fracture models proposed for quasi-static and dynamic fracture of homogeneous materials. Even though in this particular study use of the complex dynamic stress intensity factor was made in the observation of a critical state in crack face displacements, the proposed fracture criterion itself is of a more general nature. A criterion based on crack face profile may still be applicable to situations where large plasticity and/or large scale three dimensional effects are dominant or where intersonic and supersonic crack growth is occurring (e.g., in a situation where there is no K^d-dominance).

Acknowledgments

The support of ONR Grant N00014-90-J-1340 and NSF Grant MSS-9024838 is gratefully appreciated.

References

Aleksandrov, V. M. and Smetanin, B. I. (1990), Supersonic Cleavage of an Elastic Strip, *PMM* U.S.S.R., **54**(5), 677-682.

Aoki, S. and Kimura, T. (1993), Finite Element Study on the Optical Method of Caustic for Measuring Impact Fracture Toughness, *J. Mech. Phys. Solids*, **41**(3), 413-425.

Atkinson, C., Ed. (1977), Dynamic Crack Problems in Dissimilar Media, *Mechanics of Fracture - 4 : Elastodynamic Crack Problems*, Ed. G.C. Sih

Broberg, K. B. (1960), The Propagation of a Griffith Crack, *Ark. Fys.*, **18**, 159.

Broberg, K. B. (1985), Irregularities at Earth-Quake Slip, *J. Tech. Phys.*, **26**(3-4), 275-284.

Broberg, K. B. (1989), The Near-Tip Field at High Crack Velocities, *Int. J. Fract.*, **39**(1-3), 1-13.

Broberg, K. B. (1993), Intersonic Mode II Crack Expansion, private communication.

Brock, L. M. and Achenbach, J. D. (1973), Extensi[illegible] of an Interface Flaw under the Influence of Transient Waves, *Int. J. Solids Struct.*, **9**, 53-67.

Burridge, R., Conn, G. and Freund, L. B. (1979), The Stability of a Rapid Mode II Shear Crack with Finite Cohesive Traction, *J. Geophs. Res.*, **85**(B5), 2210-2222.

Bykovtsev, A. S. and Kramarovskii, D. B. (1989), Non-Stationary Supersonic Motion of a Complex Discontinuity, *PMM* U.S.S.R., **53**(6), 779-786.

Deng, X. (1992), Complete Complex Series Expansions of Near Tip Fields for Steadily Growing Interface Cracks in Dissimilar Isotropic Materials, *Engng. Fract. Mech.*, **42**(2), 237-242.

Deng, X. (1993), General Crack Tip Fields for Stationary and Steadily Growing Interface Cracks in Anisotropic Bimaterials, *J. Appl. Mech.*, **60**(1), 183-189.

Dundurs, J. (1969), Edge-bonded dissimilar orthogonal elastic wedges under normal and shear loading, *J. Appl. Mech.*, (September), 650-652.

England, A. H. (1965), A crack between dissimilar media, *J. Appl. Mech.*, 400-402.

Erdogan, F. (1965), Stress distribution in bonded dissimilar materials with cracks, *J. Appl. Mech.*, (June), 403-410.

Freund, L. B. (1990), *Dynamic Fracture Mechanics*, 1st Ed., Cambridge University Press, Cambridge.

Goldshtein, R. V. (1967), On Surface Waves in Joined Elastic Materials and their Relation to Crack Propagation along the Junction, *Appl. Math. Mech.*, **31**, 496-502.

Hutchinson, J. W. (1989), Mixed mode fracture mechanics of interfaces, Harvard University Report.

Lambros, J., Liu, C. and Rosakis, A. J. (1994), Intersonic Decohesion of Interfaces: Theory and Experiments, in preparation.

Lambros, J. and Rosakis, A. J. (1994), On the Investigation of Dynamic Decohesion Criteria in Jointed Structures, in preparation.

Lee, Y. J. and Rosakis, A. J. (1993), Interfacial Cracks in Plates : A Three Dimensional Numerical Investigation, *Int. J. Solids Struct.*, **30**(22), 3139-3158.

Liechti, K. M. and Chai, Y. S. (1991), Biaxial Loading Experiments for Determining Interfacial Fracture-Toughness, *J. Appl. Mech.*, **58**(3), 680-687.

Liechti, K. M. and Chai, Y. S. (1992), Asymmetric Shielding in Interfacial Fracture under Inplane Shear, *J. Appl. Mech.*, **59**(2), 295-304.

Liu, C., Lambros, J. and Rosakis, A. J. (1993), Highly Transient Elastodynamic Crack Growth in a Bimaterial Interface : Higher Order Asymptotic Analysis and Experiments, *J. Mech. Phys. Solids.*, **41**(12), 1887-1954.

Lo, C. Y., Nakamura, T. and Kushner, A. (1993), Computational Analysis of Dynamic Crack Propagation Along Bimaterial Interfaces, to appear in *J. Mech. Phys. Solids*.

Mason, J. J., Lambros, J. and Rosakis, A. J. (1992), The use of a Coherent Gradient Sensor in dynamic mixed-mode fracture mechanics experiments, *J. Mech. Phys. Solids.*, **40**(No. 3), 641-661.

Nakamura, T. (1991), Three Dimensional Stress Fields of Elastic Interface Cracks, *J. App. Mech.*, **58**(4), 939-946.

Nakamura, T., Kushner, A. and Lo C. Y., (1994), Interlaminar Dynamic Crack Propagation, special issue of *Int. J. Solids Struct.* devoted to "Failure Mechanics of Modern Materials", (A. J. Rosakis, A. Shukla, guest editors).

Rice, J. R. (1988), Elastic fracture mechanics concepts for interfacial cracks, *J. App. Mech.*, **55**(March), 98-103.

Rice, J. R. and Sih, G. C. (1965), Plane problems of cracks in dissimilar media, *J. of App. Mech.*, (June), 418-423.

Rosakis, A. J. (1993), Two optical techniques sensitive to gradients of optical path difference: The method of caustics and the coherent gradient sensor (CGS), *Experimental techniques in fracture*, Ed. J. Epstein, 327-425.

Rosakis, A. J., Lee, Y. J. and Lambros, J. (1991), Dynamic crack growth in bimaterial interfaces, ASME, Atlanta, GA, AMD-Vol.130, *Experiments in Micromechanics of Failure Resistant Materials*, Ed. K.-S. Kim.

Shih, C. F. (1991), Cracks on Bimaterial Interfaces : Elasticity and Plasticity Aspects, Matls. Science Engng., **A143**, 77-90.

Sih, G. C. and Rice, J. R. (1964), Bending of Plates of Dissimilar Materials with Cracks, *J. App. Mech.*, **31**, 477-482.

Tippur, H. V., Krishnaswamy, S. and Rosakis, A. J. (1991), A Coherent Gradient Sensor for crack tip measurements : Analysis and experimental results, *Int. J. Fract.*, **48**, 193-204.

Tippur, H. V. and Rosakis, A. J. (1991), Quasi-static and Dynamic Crack Growth along Bimaterial Interfaces : A note on Crack-Tip Field Measurements using Coherent Gradient Sensing, *Exp. Mech.*, **31**(No. 3), 243-251.

Williams, M. L. (1959), The stresses around a fault or crack in dissimilar media, *Bulletin of the Seismological Society of America*, **49**(No. 2), 199-204.

Willis, J. R. (1971), Fracture Mechanics of Interfacial Cracks, *J. Mech. Phys. Solids*, **19**, 353-368.

Willis, J. R. (1973), Self-Similar Problems in Elastodynamics, *Phil. Trans. R. Soc. Lond.*, **274**, 435-491.

Wu, K. C. (1991), Explicit Crack Tip Fields of an Extending Interface Crack in an Anisotropic Bimaterial, *Int. J. Solids Struct.*, 27(4), 455-466.

Yang, W., Suo, Z. and Shih, C. F. (1991), Mechanics of Dynamic Debonding, *Proc. R. Soc. Lond.*, **A433**, 679-697.

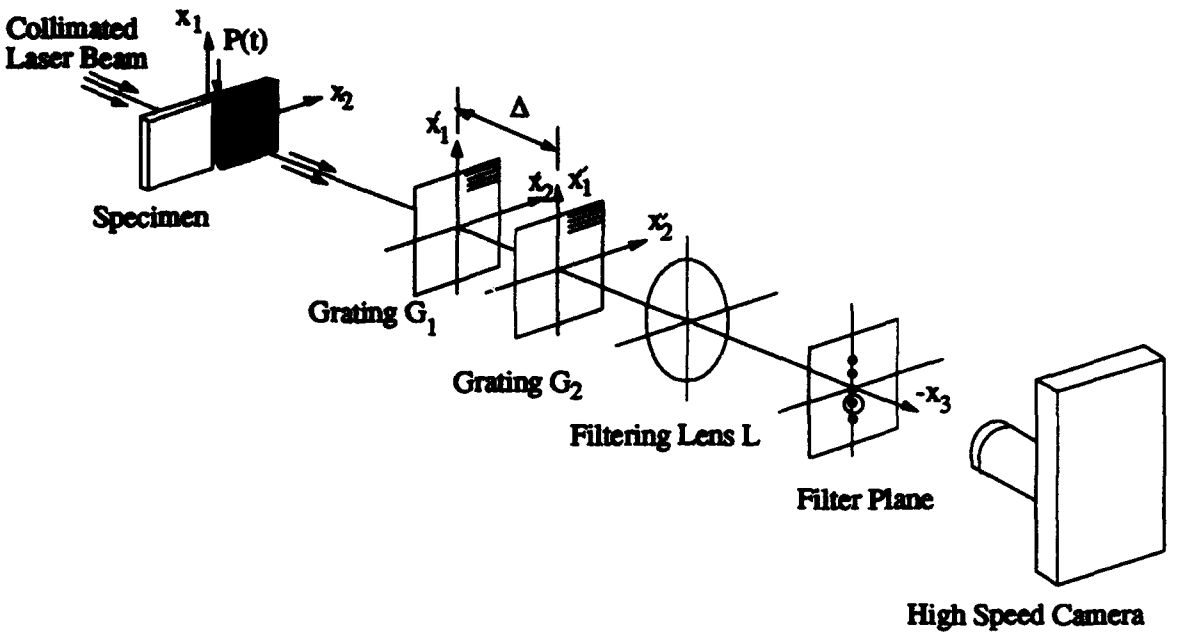

Figure 1: Schematic of CGS set-up in transmission.

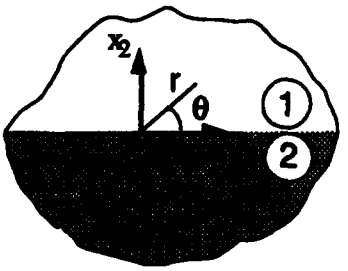

Figure 2: Geometry of interfacial crack problem.

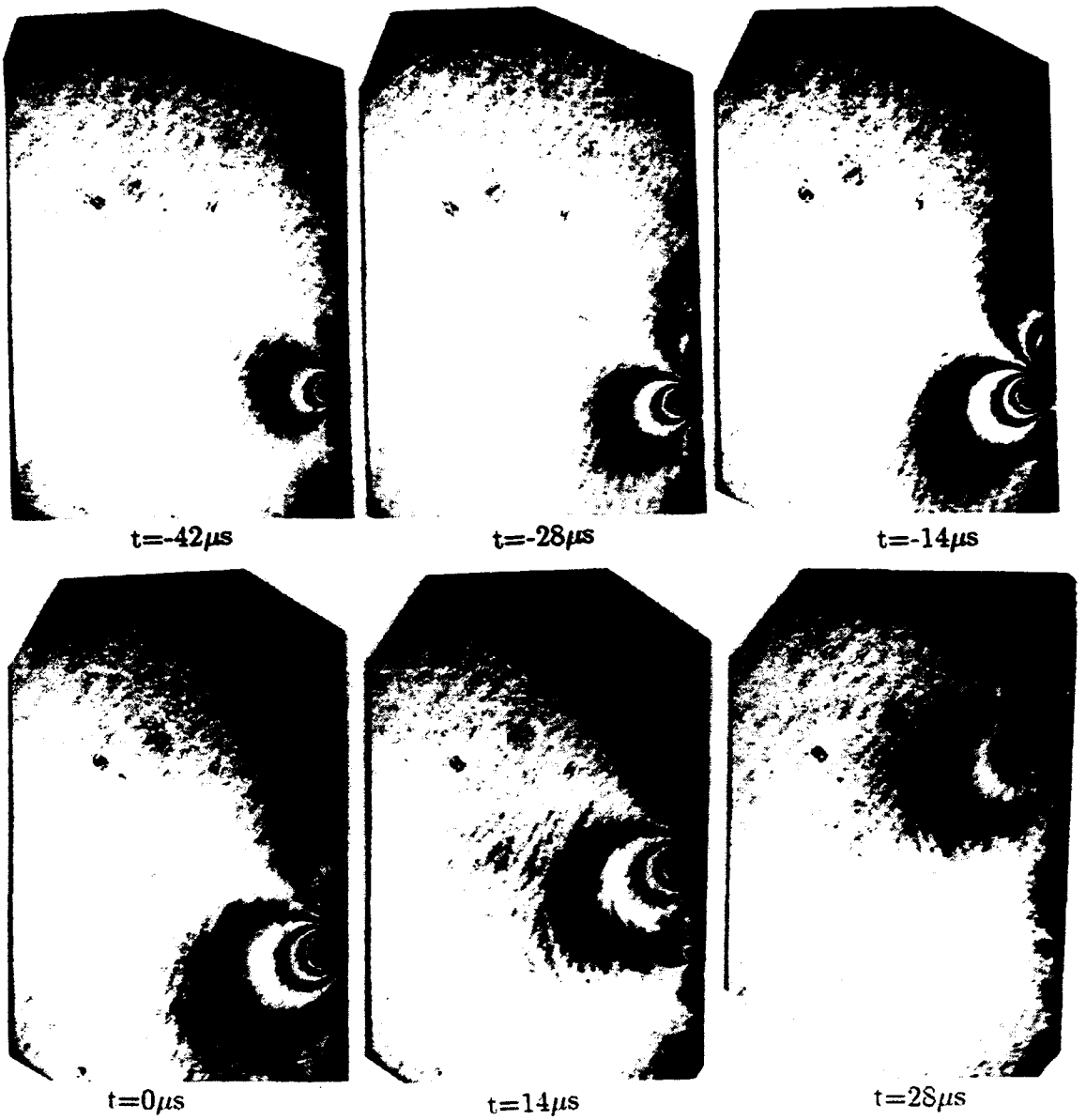

Figure 3 : Selected sequence of CGS interferograms from a PMMA/aluminum three point bend drop weight tower test (from Tippur and Rosakis (1991)).

t=9.5 μs
v=640 m/s

t=16.5 μs
v=790 m/s

t=23 μs
v=800 m/s

t=32 μs
v=880 m/s

Figure 4 : Selected sequence of CGS interferograms from a one point bend PMMA/steel drop weight tower test.

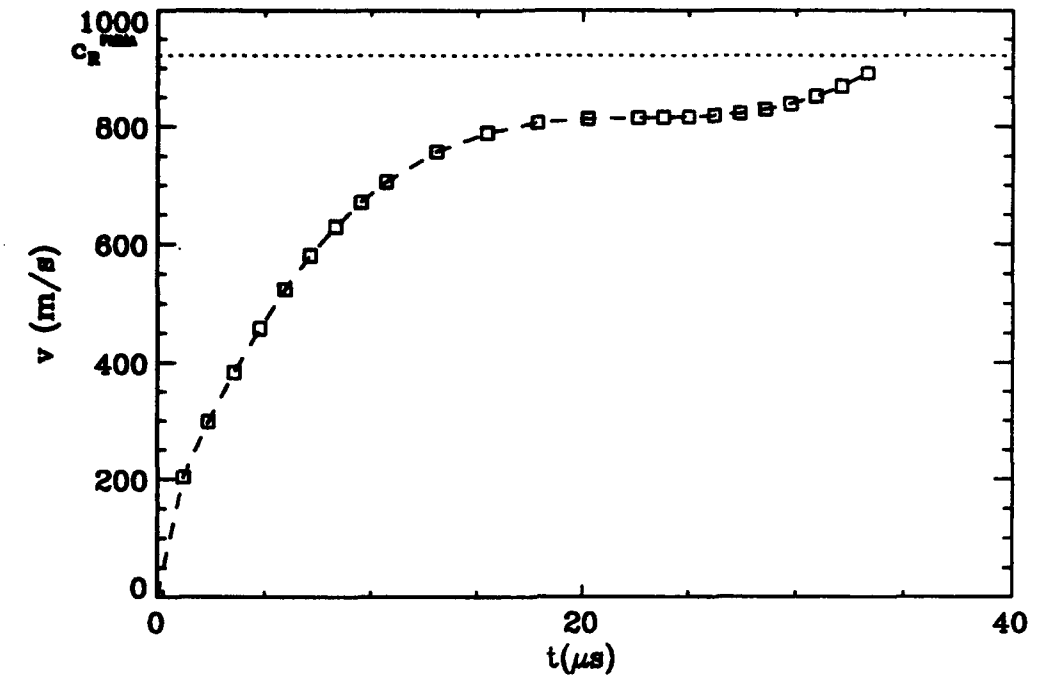

(a)

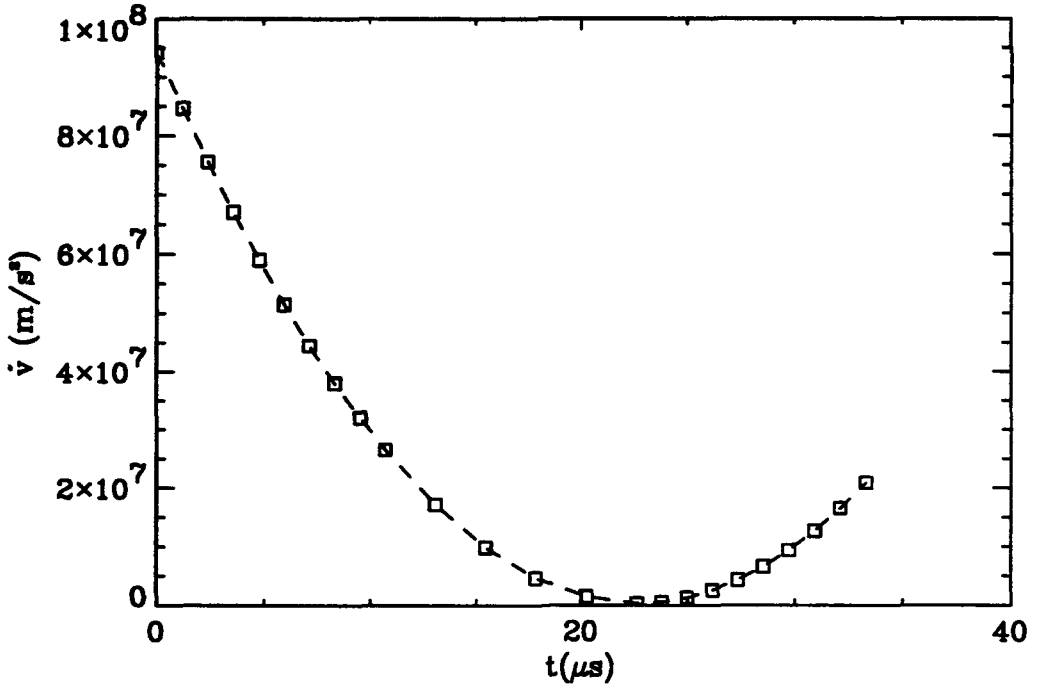

(b)

Figure 5: Velocity, (a) and acceleration, (b) time histories for the experiment shown in figure 4.

t=3 μs
v=140 m/s

t=8 μs
v=720 m/s

t=13 μs
v=1100 m/s

t=16.5 μs
v=1100 m/s

Figure 6: Selected sequence of CGS interferograms obtained from a one point bend air gun test on a PMMA/steel specimen.

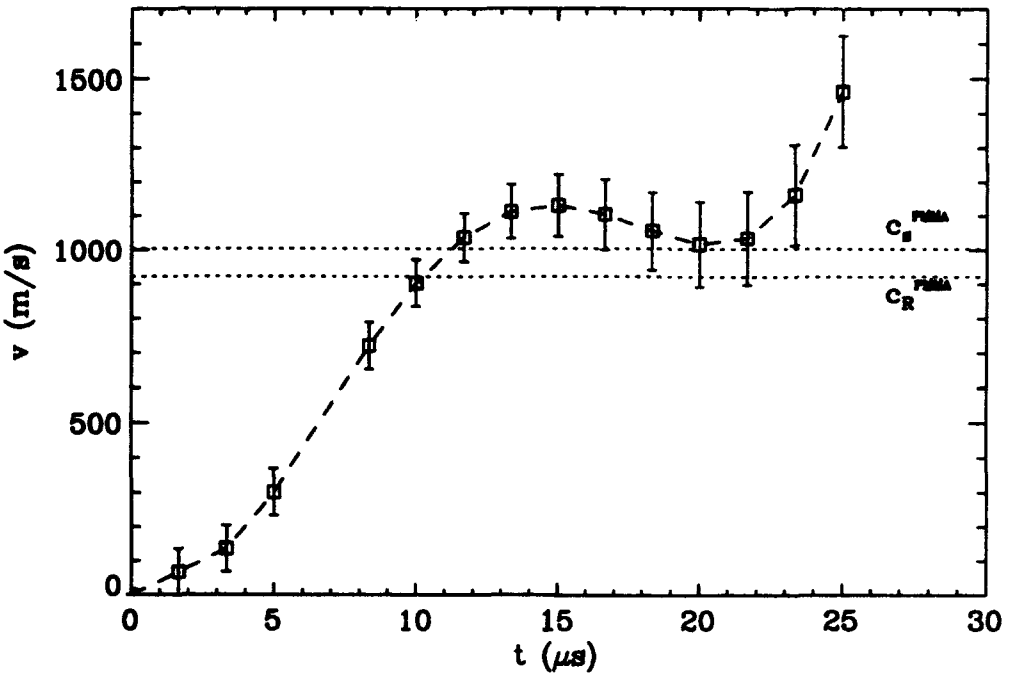

(a)

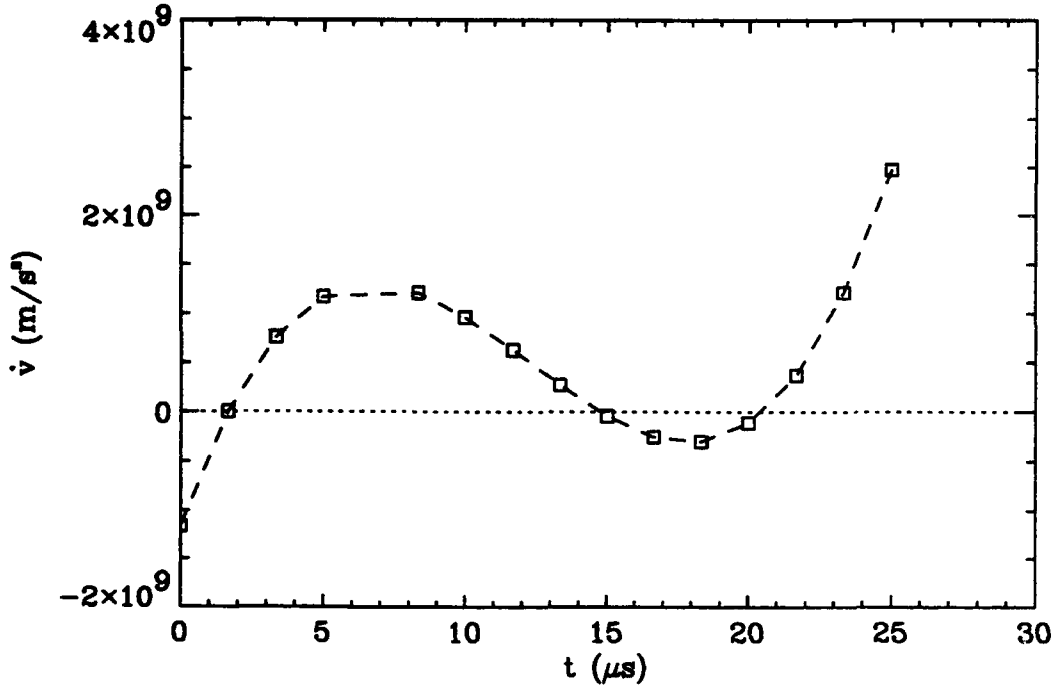

(b)

Figure 7: Velocity, (a) and acceleration, (b) time histories for the experiment shown in figure 6.

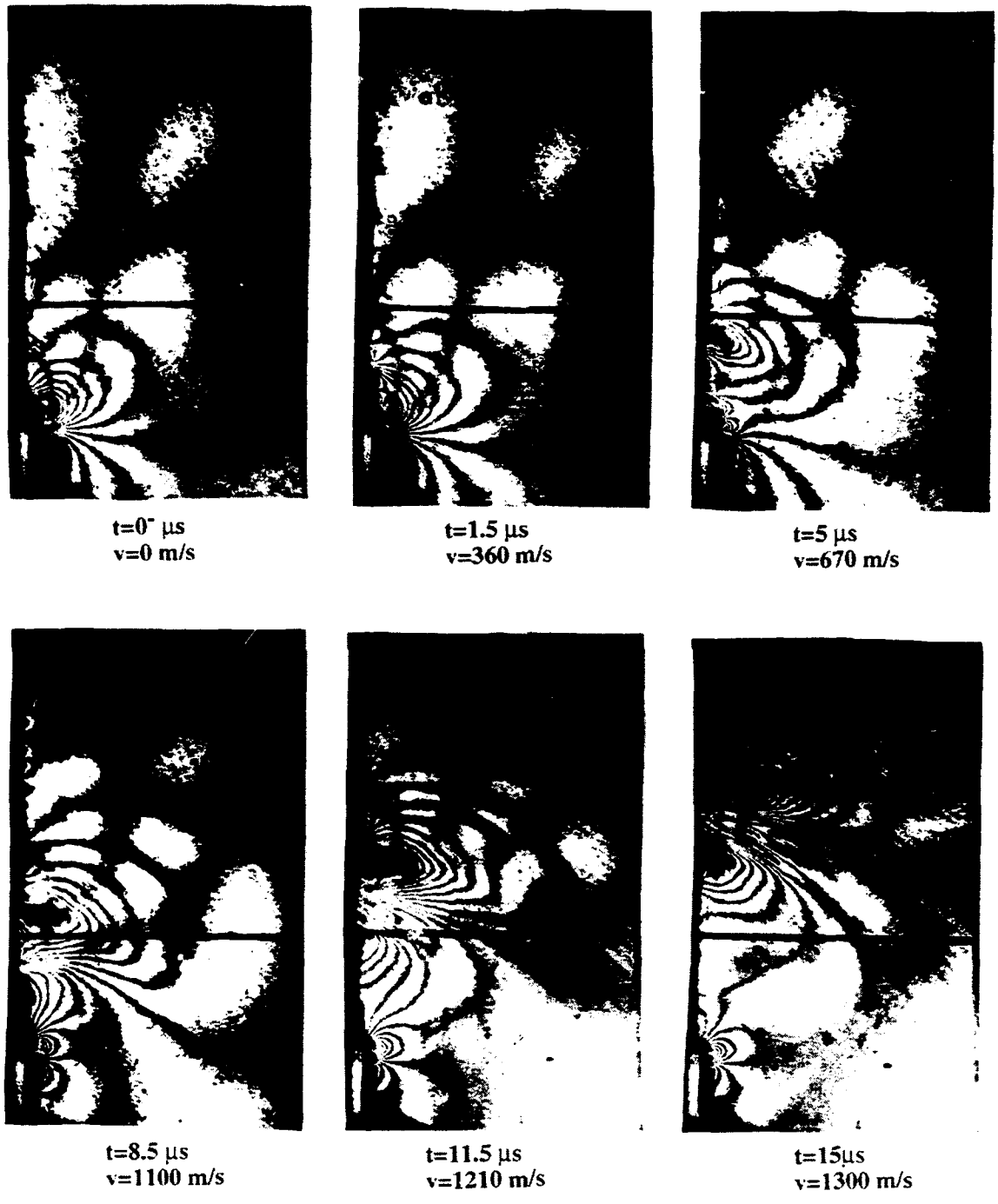

Figure 8: Selected sequence of CGS interferograms of a growing crack in a one point bend PMMA/steel air gun experiment (blunt starter notch).

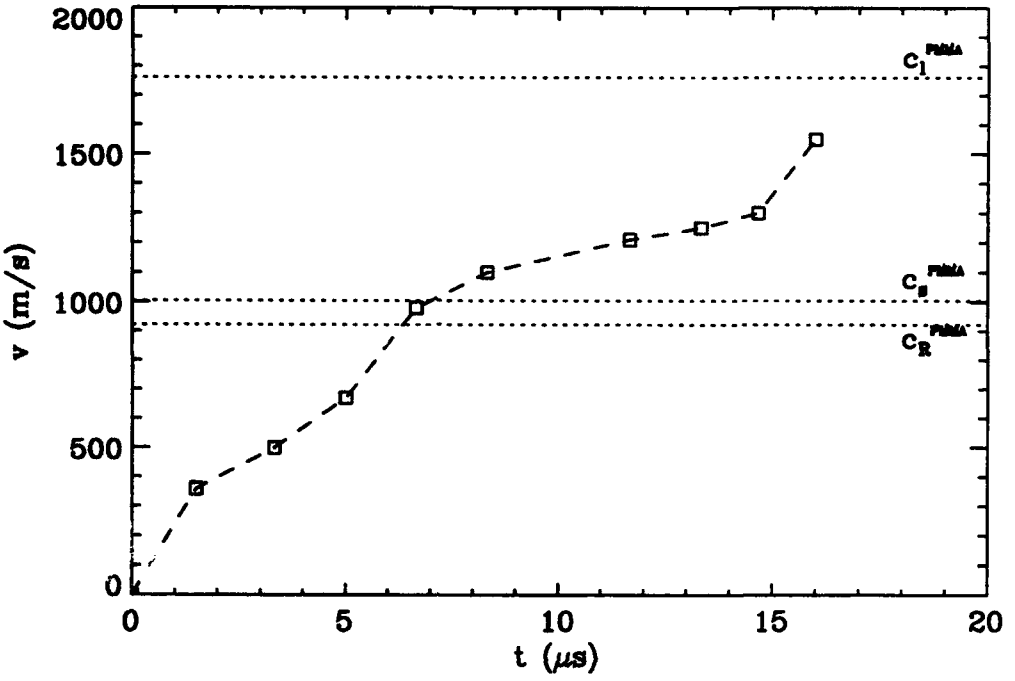

Figure 9: Velocity time history for the experiment shown in figure 8.

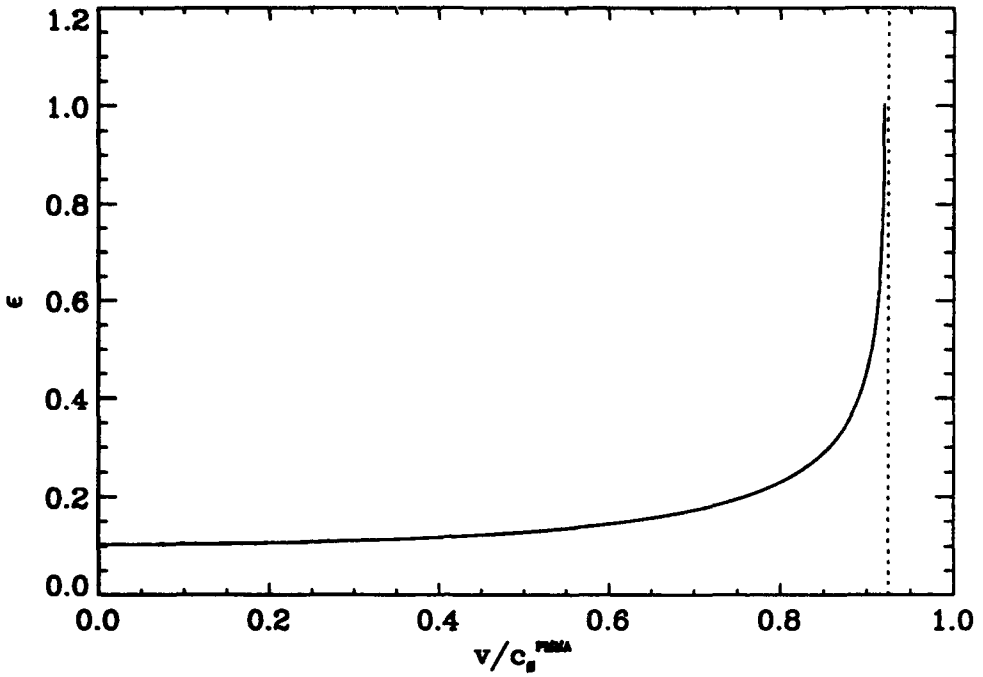

Figure 10: Variation of oscillatory index with velocity for a PMMA/steel bimaterial system (plane stress conditions).

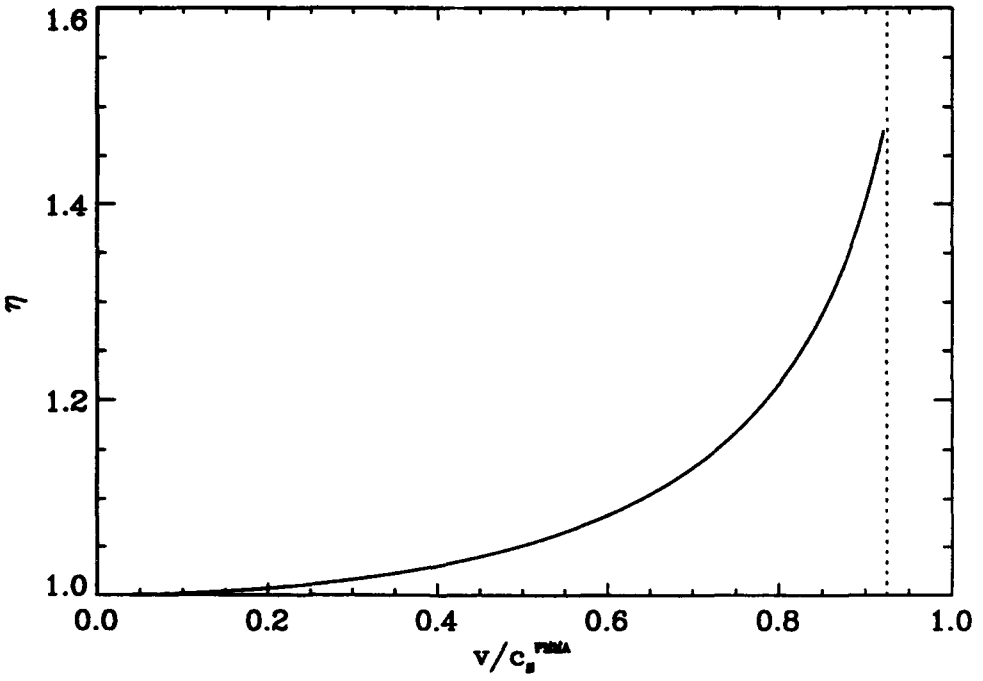

Figure 11: Variation of traction resolution factor with velocity for a PMMA/steel bimaterial system (plane stress conditions).

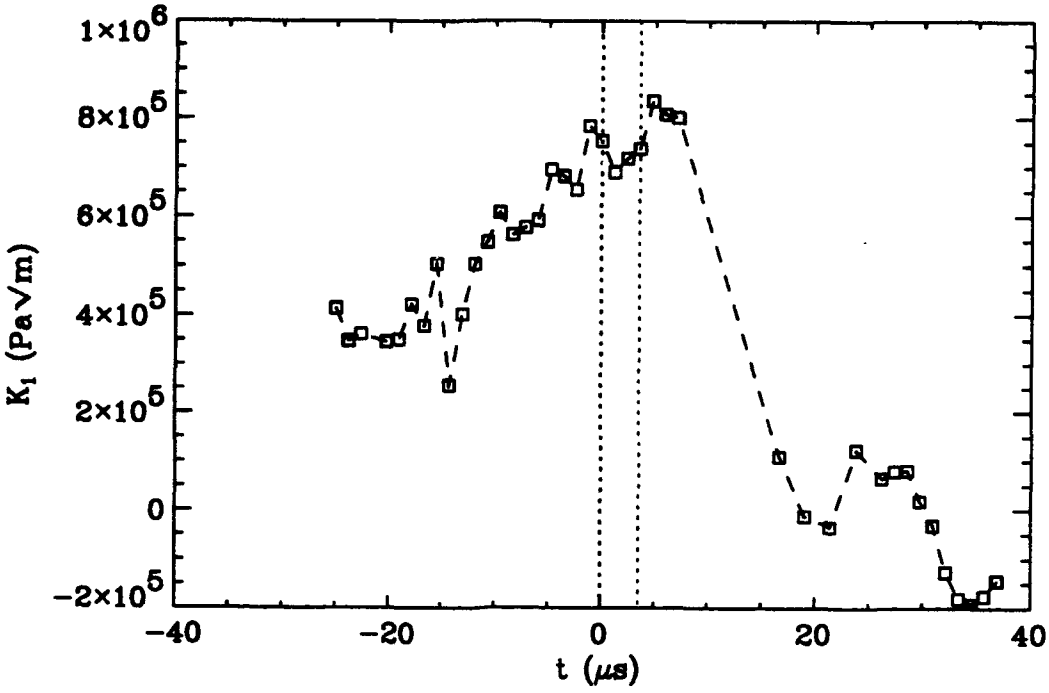

(a)

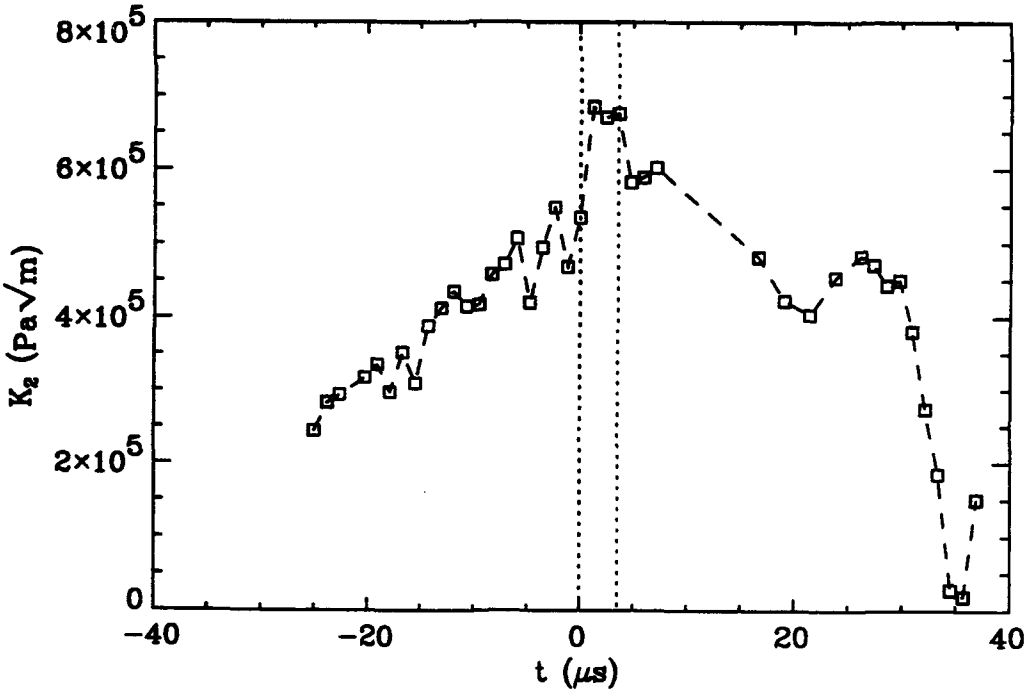

(b)

Figure 12(a,b): Time history of components of complex stress intensity factor for the experiment shown in figure 4.

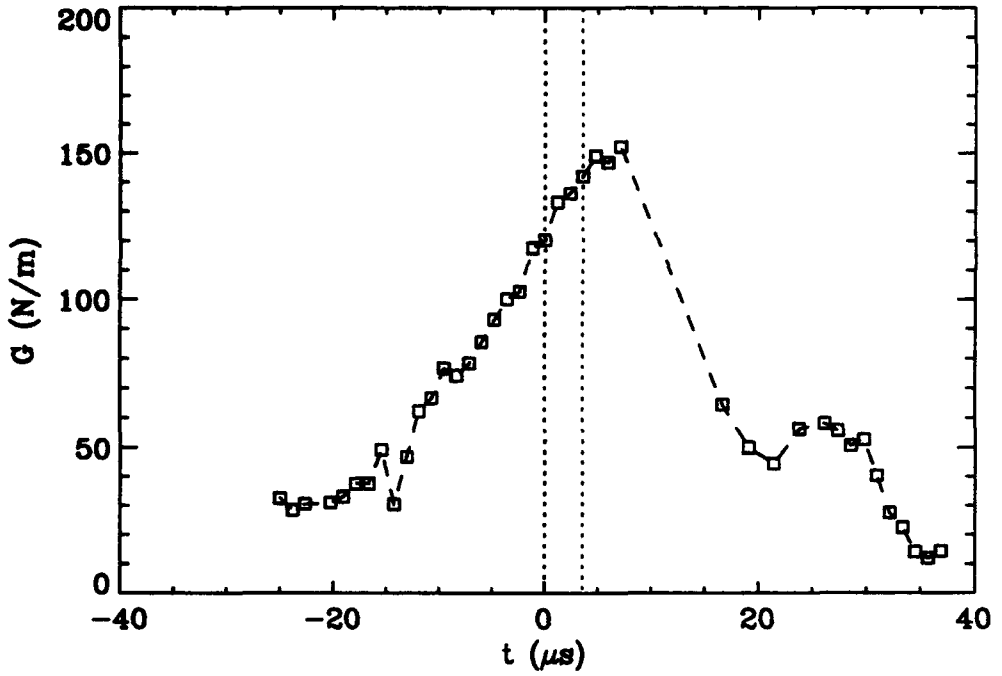

(a)

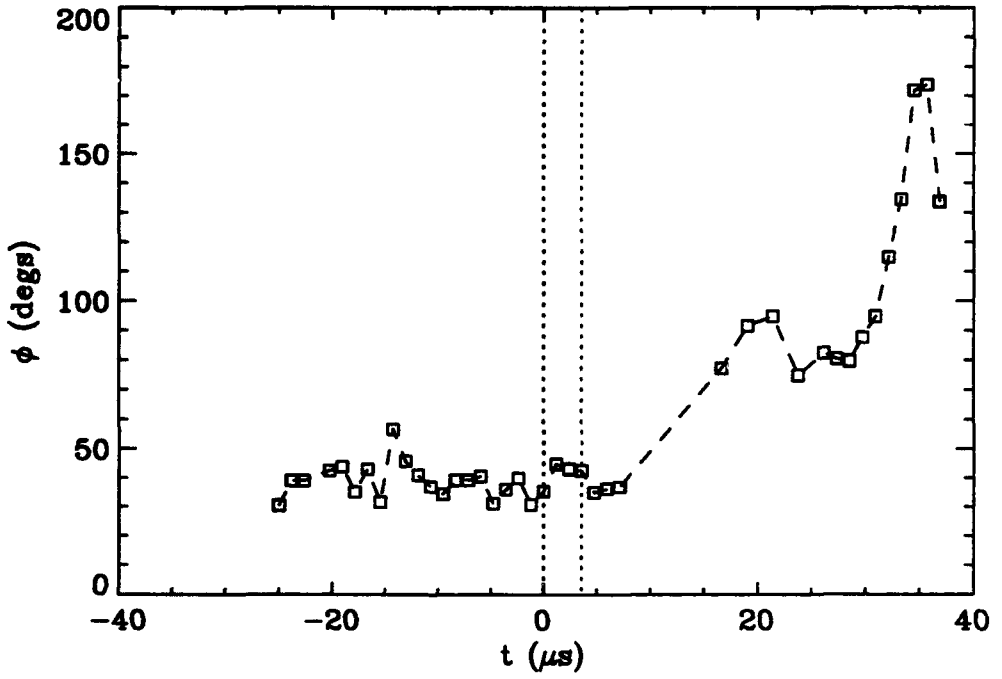

(b)

Figure 13(a,b): Time history of energy release rate and phase angle (L=1m) for the experiment shown in figure 4.

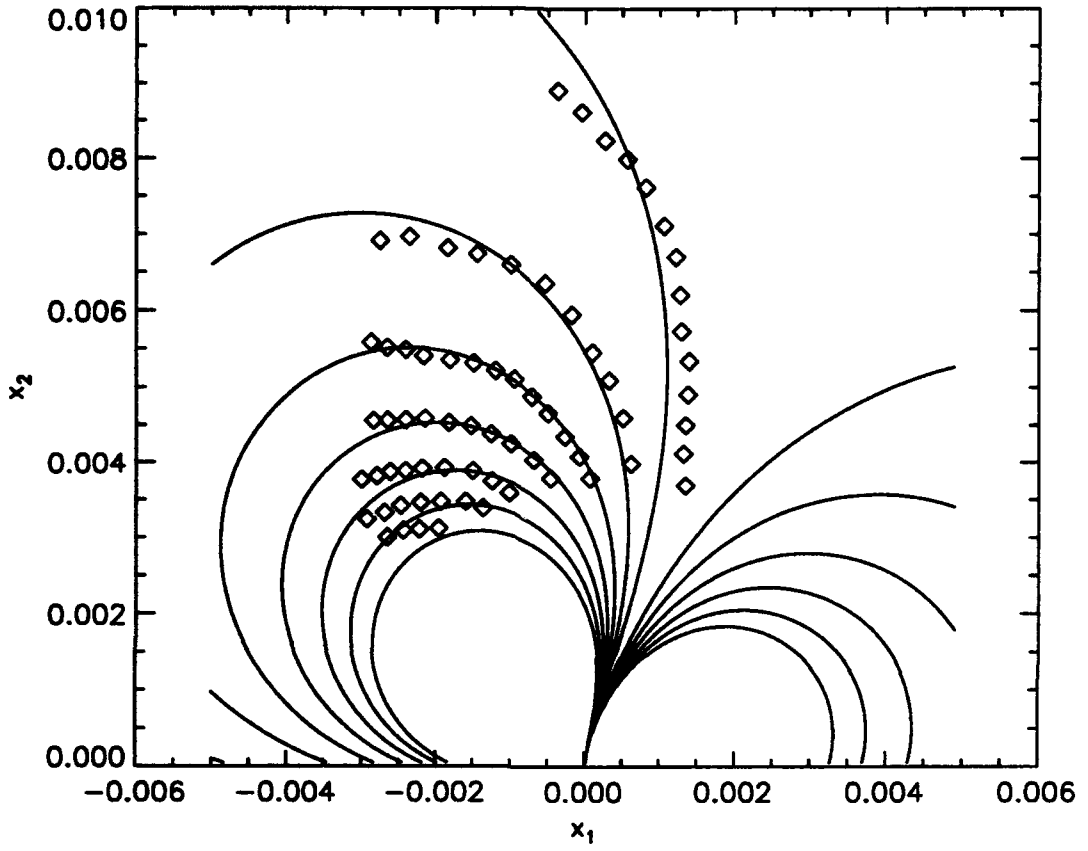

Figure 14: Illustration of collapse of K^d-field in inner fringes at times slightly after initiation.

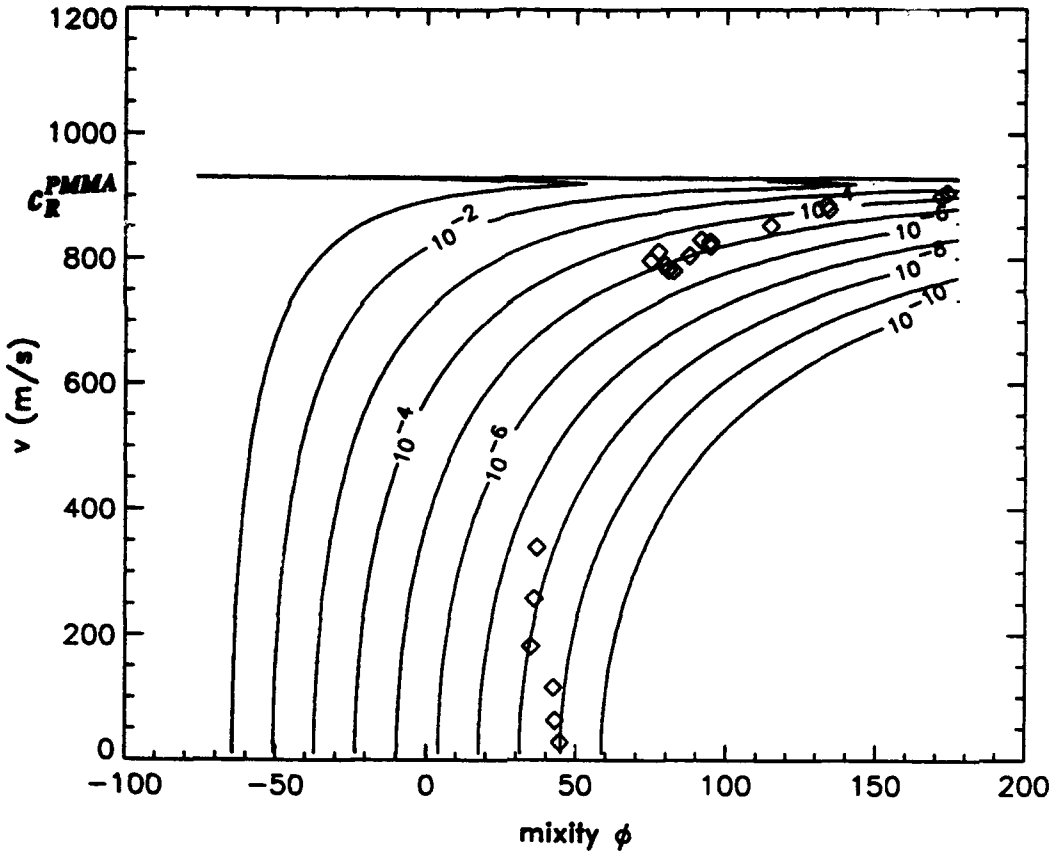

Figure 15: Magnitude of predicted contact zone in PMMA/steel one point bend drop weight tower experiment shown in figure 4.

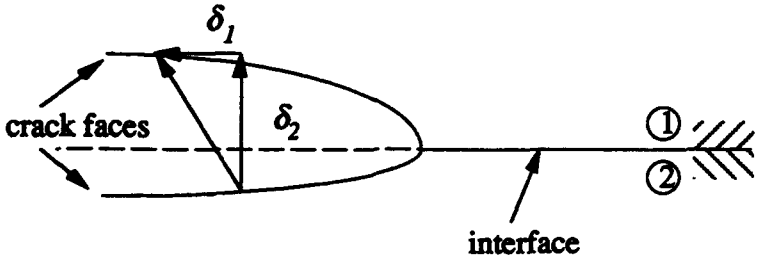

Figure 16: Schematic definition of opening and shearing displacements behind the interfacial crack tip.

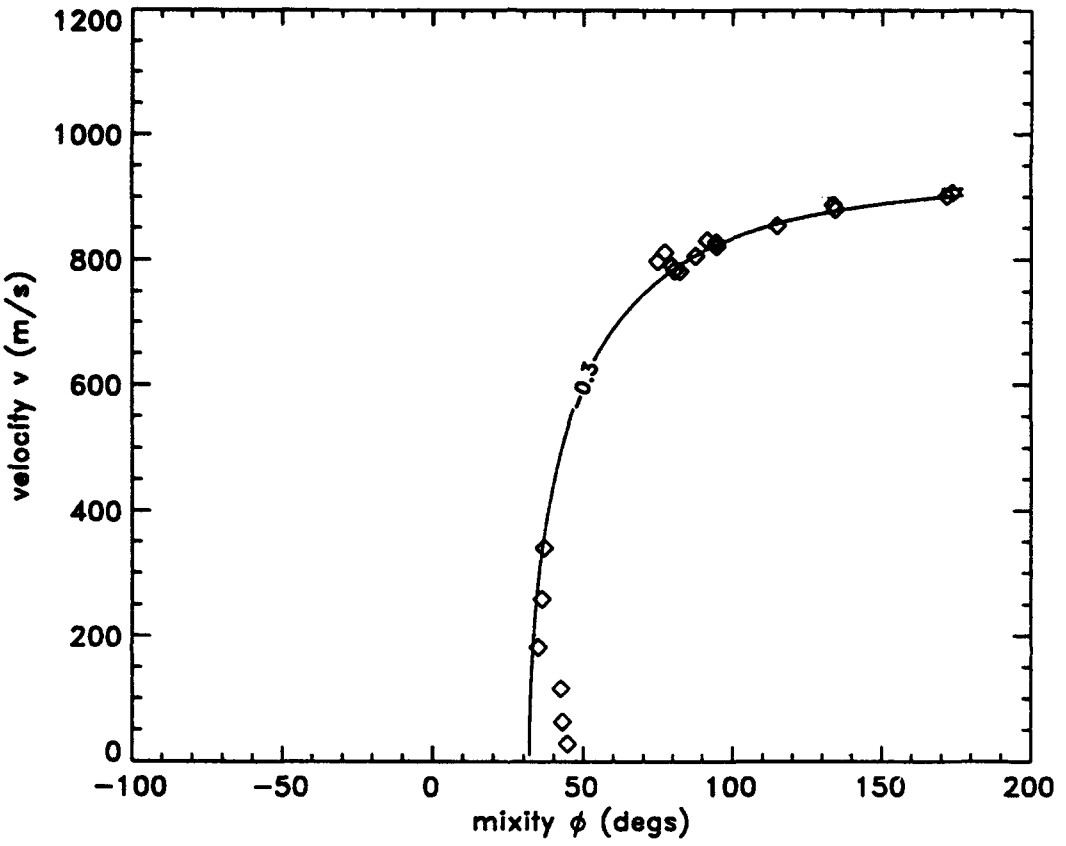

Figure 17: Fit of equation (14) to experimental data from the one point bend PMMA/steel drop weight tower test shown in figure 4.

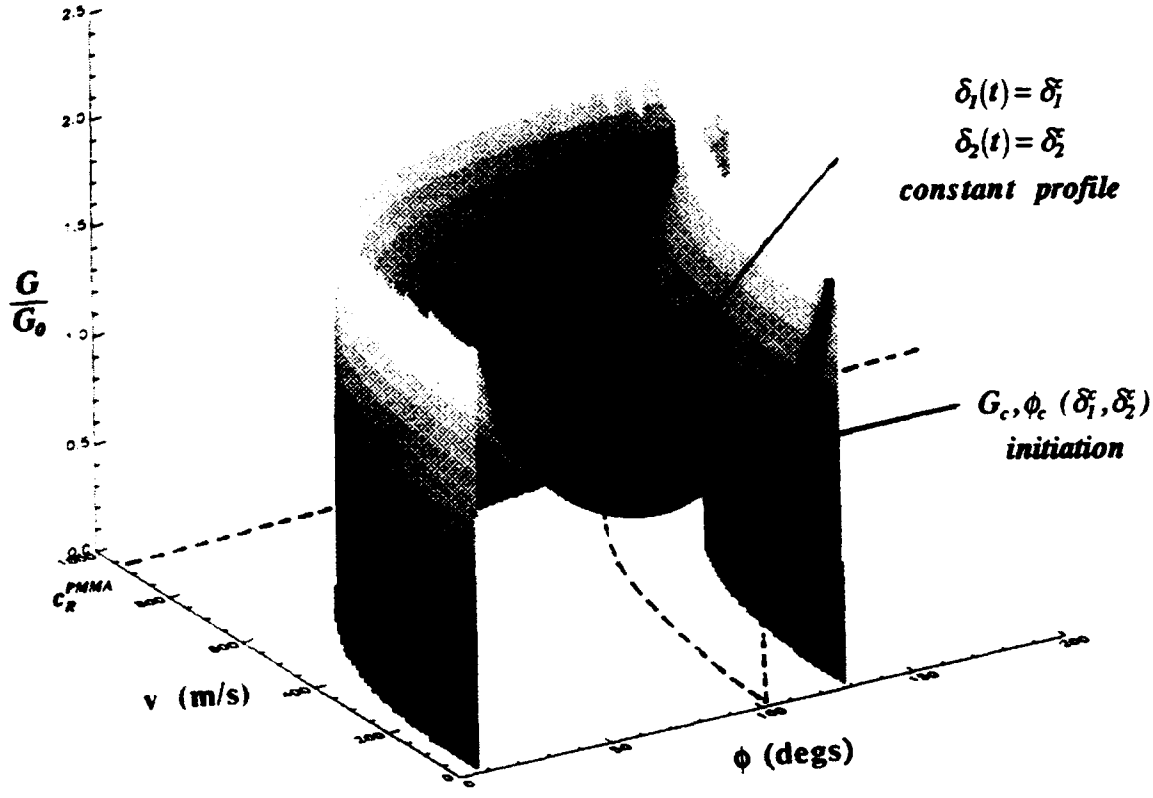

Figure 18: (G, v, f) surface for the quantity $\delta_2(t)\big|_{r=a} = const.$. Crack path corresponding to constant crack face profile is superposed.

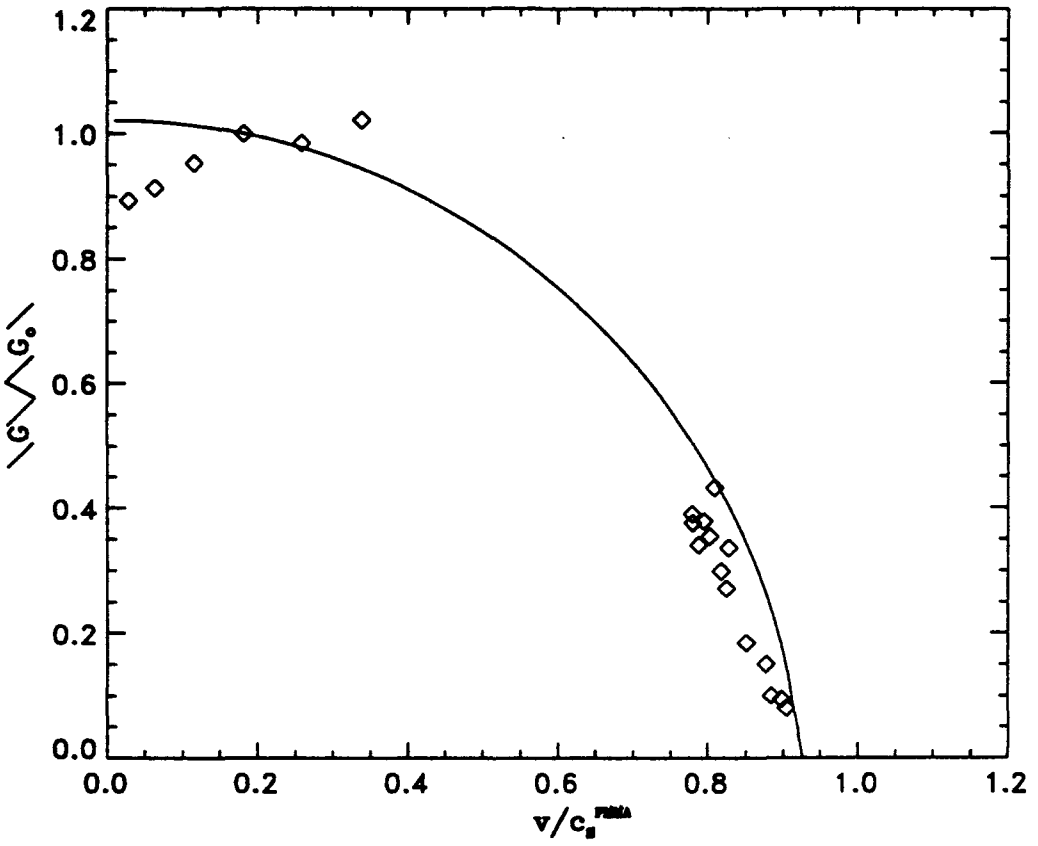

Figure 19: Comparison of normalized energy release rate from the PMMA/steel drop weight tower experiment with the prediction of constant crack profile growth (equation (17)).

PROPERTY	PMMA	6061-T6 Aluminum	AISI 4340 Steel
E (GPa)	3.24	80	208
ν	0.35	0.33	0.3
c_d (m/s)	2080	6600	5970
c_s (m/s)	1000	3330	3190
c_R (m/s)	935	3100	2950
ρ (Kgr/m^3)	1190	2710	7830
$\varepsilon^{P/A} = 0.0981$	$\varepsilon^{P/S} = 0.1037$		$\varepsilon^{P/R} = 0.1073$

Table 1: Mechanical properties of interface constituents.

UNITY CLASSIFICATION OF THIS PAGE

REPORT DOCUMENTATION PAGE

Form Approved
OMB No. 0704-0188

REPORT SECURITY CLASSIFICATION Unclassified	1b. RESTRICTIVE MARKINGS
SECURITY CLASSIFICATION AUTHORITY	3. DISTRIBUTION/AVAILABILITY OF REPORT
DECLASSIFICATION/DOWNGRADING SCHEDULE	
PERFORMING ORGANIZATION REPORT NUMBER(S) SM Report 94-2	5. MONITORING ORGANIZATION REPORT NUMBER(S)
NAME OF PERFORMING ORGANIZATION Graduate Aeronautical Labs. California Institute of Tech.	6b. OFFICE SYMBOL (If applicable)
	7a. NAME OF MONITORING ORGANIZATION ONR
ADDRESS (City, State, and ZIP Code) Caltech 105-50 Pasadena, CA 91125	7b. ADDRESS (City, State, and ZIP Code)
NAME OF FUNDING/SPONSORING ORGANIZATION ONR	8b. OFFICE SYMBOL (If applicable)
	9. PROCUREMENT INSTRUMENT IDENTIFICATION NUMBER ONR N00014-90-J-1340
ADDRESS (City, State, and ZIP Code) Dr. Y. Rajapakse, Scientific Officer ONR, Code 1132 SM 800 N. Quincy St., Arlington, VA 22217-5000	10. SOURCE OF FUNDING NUMBERS PROGRAM ELEMENT NO. / PROJECT NO. / TASK NO. / WORK UNIT ACCESSION NO.

TITLE (Include Security Classification)
Dynamic Decohesion of Bimaterials : Experimental Observations and Failure Criteria

PERSONAL AUTHOR(S)
John Lambros and Ares J. Rosakis

TYPE OF REPORT	13b. TIME COVERED	14. DATE OF REPORT (Year, Month, Day)	15. PAGE COUNT
	FROM _____ TO _____	February 1994	49

SUPPLEMENTARY NOTATION
Submitted for publication in the International Journal of Solids and Structures

COSATI CODES			18. SUBJECT TERMS (Continue on reverse if necessary and identify by block number)
FIELD	GROUP	SUB-GROUP	

ABSTRACT (Continue on reverse if necessary and identify by block number)

Some results of high speed interferometric measurements on dynamically interfacial cracks are presented. PMMA/steel bimaterial specimens of the one point bend type are used. They are impact loaded using either a drop weight tower device or a high speed gas gun. This results in two distinct groups of experiments at different loading rates. In all cases very high crack propagation speeds are seen. In gas gun experiments, terminal crack tip speeds of up to $1.5c_s^{PMMA}$, where c_s^{PMMA} is the shear wave speed of PMMA, are measured. In addition, high accelerations (10^7g, where g is the acceleration of gravity) are observed and reported. Theoretically predicted near tip fields are used to extract experimental values of the dynamic complex stress intensity factor histories in each test. Using the fitted histories of the complex stress intensity factor, a dynamic crack growth criterion relating the energy release rate to phase angle and crack tip velocity is proposed and discussed.

DISTRIBUTION/AVAILABILITY OF ABSTRACT ☐ UNCLASSIFIED/UNLIMITED ☒ SAME AS RPT. ☐ DTIC USERS	21. ABSTRACT SECURITY CLASSIFICATION Unclassified
NAME OF RESPONSIBLE INDIVIDUAL	22b. TELEPHONE (Include Area Code) / 22c. OFFICE SYMBOL

Form 1473, JUN 86 Previous editions are obsolete. SECURITY CLASSIFICATION OF THIS PAGE